KERNFORSCHUNGSZENTRUM

KARLSRUHE

Juli 1974 KFK 2028

Institut für Angewandte Systemtechnik und Reaktorphysik
Projekt Schneller Brüter

Physics Investigations of Sodium Cooled Fast Reactors SNEAK-Assembly 9A

M. Pinter

GESELLSCHAFT
FÜR
KERNFORSCHUNG M.B.H.

KARLSRUHE

GESELLSCHAFT FÜR KERNFORSCHUNG M. B. H.
KARLSRUHE

KERNFORSCHUNGSZENTRUM KARLSRUHE

1974 KFK 2028

Institut für Angewandte Systemtechnik und Reaktorphysik

Projekt Schneller Brüter

Physics Investigations of Sodium Cooled Fast Reactors

SNEAK-Assembly 9A

M. Pinter

With contributions from

R. Böhme, G. Durance[1], P. Fehsenfeld, E.A. Fischer, F. Helm, E. Korthaus, S. Pilate[2], A. Raberain-Elbel, W. Scholtyssek, D. Wintzer, G. Wittek

1) Delegate from AAEC, Sydney, Australia

2) Belgonucleaire, Brussels

Gesellschaft für Kernforschung mbH., Karlsruhe

Physics Investigations of Sodium Cooled Fast Reactors

SNEAK-Assembly 9A

Abstract

The series of assemblies which were built for investigations with regard to the SNR was continued with the assembly SNEAK-9A. This assembly was a mock up of the SNR with two core zones in the radial direction. The fuel material was enriched uranium. The main objectives were criticality prediction, determination of the control rod worth and the measurement of the power distribution. The assembly was built up in three steps: SNEAK-9A-0, a clean core; SNEAK-9A-1, a core with 12 simulated control rods filled with sodium follower material; and SNEAK-9A-2, the final mock up core with control rods partially inserted. In this report the results of the more physical investigations, i.e. criticality, reaction rate and reactivity worth measurements are given. An other report will describe the results directly related to the simulated SNR control rods.

15.7.1974

Physikalische Untersuchungen an natrium-gekühlten schnellen Reaktoren

Anordnung SNEAK-9A

Zusammenfassung

Die Reihe der Anordnungen, die im Zusammenhang mit Untersuchungen für den SNR aufgebaut wurden, wurde mit dem SNR-mock-up SNEAK-9A fortgesetzt. Das Core bestand aus zwei verschieden angereicherten radialen Zonen mit Uran als Brennstoff. Hauptgegenstände der Untersuchungen waren die Bestimmung der Kritikalität, der Kontrollstabwerte und der Leistungsverteilung. Die Anordnung wurde in drei Schritten aufgebaut: SNEAK-9A-0, ein Core ohne Kontrollstäbe; SNEAK-9A-1, ein Core mit 12 simulierten Kontrollstäben, die alle mit Natrium Nachfolgermaterial gefüllt waren; und SNEAK-9A-2, das endgültige mock up Core mit teilweise eingefahrenen Kontrollstäben. Dieser Bericht enthält die Ergebnisse der mehr physikalischen Untersuchungen: Kritikalität, Reaktionsraten- und Materialwertmessungen. In einem zweiten Bericht werden alle Ergebnisse zusammengefaßt, die unmittelbar mit den simulierten SNR-Kontrollstäben zusammenhängen.

Table of contents

1. Introduction

The series of assemblies which were built for investigations with regard to the SNR (Schneller Natriumgekühlter Reaktor) /1/, /2/, /3/, /4/ was continued with the assembly SNEAK-9A.

This assembly was a mock up of the SNR, with two core zones in the radial direction. The fuel material was enriched uranium.

The main objectives were:

- comparison of experimental and calculated k_{eff}
- measurement of the reactivity worth of the simulated SNR control rods
- measurement of the power distribution for different configurations of the simulated control rods.

To solve these problems as accurately as possible it seemed expedient to built up SNEAK-9A in three steps:

SNEAK-9A-0 was a clean core without simulated control rods. It was built for some basic investigations with the main purpose to check the calculation methods for an uranium core.

SNEAK-9A-1 was a mock up of the end of life state of the SNR. That means, all twelve control rod positions are filled with sodium follower material in the core region and absorber in the upper axial blanket (simulation of withdrawn control rods).

SNEAK-9A-2 simulated a possible "beginning of life configuration" of the SNR. Nine of the twelve control rods were partially inserted. Most of the investigations, namely the power distribution measurements and the control rod reactivity worth measurements were performed in this assembly.

Design and evaluation of the experiments were performed in close cooperation between the Institut für Angewandte Systemtechnik und Reaktorphysik of the Kernforschungszentrum Karlsruhe and the industrial consortium for the construction of the SNR. Some experiments were also evaluated by French scientists of the fast critical facility MASURCA at Cadarache.

This report describes the results of the basic experiments performed in SNEAK-9A-0 and the k_{eff}-calculations for all SNEAK-9A assemblies. Another report will document the results of the control rod worth measurements, the power distribution measurements, and the detailed calculation methods used for the evaluation of these experiments /5/.

2. Description of the assemblies

2.1 General characteristics of the assemblies

All the SNEAK-9A assemblies, 9A-0, 9A-1 and 9A-2 contained two cylindrical core regions with a height of 90.0 cm, a radial blanket about 30 cm thick, and an upper and lower axial blanket 40.8 cm thick. Both axial blankets were subdivided into two parts with different material compositions.

In designing the unit cells for SNEAK-9A an effort was made to approach the compositions and spectra in the respective zones of the SNR as well as possible. However, the cell also had to be kept reasonably simple in order to allow a meaningful interpretation, in particular of the reaction rate measurements. As a fuel, 20.04% enriched uranium was used in the inner zone and 35.28% enriched uranium in the outer zone. Fig. 1 and 2 show the unit cells and the structure of the elements of the inner and outer core zone.

Fig. 3 and 4 show the structure of the SNEAK control rods (shim- and safety rods), and the cells used. In designing these cells attention was payed to get approximately the same material buckling as for the normal cells.

In the axial blanket a breeder composition was approximated. Because of the lack of UO_2 platelets this had to be done using two different unit cells. Over a thickness of about 20 cm immediately adjacent to the core a composition containing mainly UO_2 and Na was used (inner axial blanket). For the remaining part of the blanket a cell containing natural uranium, Al_2O_3, Al, and stain-

less steel was used (outer axial blanket). The blanket cells are also shown in Fig. 1 and 2 and for the SNEAK control rods in Fig. 3 and 4.

The radial blanket consisted of depleted uranium with a content of 0.41% ^{235}U.

2.2 Description of the assembly SNEAK-9A-0

SNEAK-9A-0 was a two zone core without any simulated control rods of the SNR. Fig. 6 shows the horizontal cross section of the realized critical configuration and a vertical cross section through one quarter of the equivalent cylindrical core. To define the radii of this core it was assumed that the areas of the real and the cylindrical core cross sections are equal.

In designing the core attention was given to get a central zone without any SNEAK control rods. This is favourable to an accurate evaluation of the buckling measurement (see section 8.). The radius of this zone is about 27 cm.

2.3 Description of the assemblies SNEAK-9A-1 and SNEAK-9A-2

The main characteristic of these assemblies is that they contain simulated SNR control rods. There were twelve SNR control rod positions, which were divided into 3 groups:

- RT1 consisting of three control rods positioned in the inner core zone at about one third of the core radius.

- RT2 consisting of six control rods positioned in the outer core zone but directly adjacent to the inner core zone.

- A secondary shut-down system, consisting of three rods, positioned in the inner core zone between RT1 and RT2.

Each simulated control rod consisted of four SNEAK elements. To be able to adapt its reactivity worth as accurately as possible to a given value, the SNEAK elements were filled in the absorber part with a pattern of four by four rodlets part of which were B_4C filled aluminium tubes, the rest consisting of solid aluminium. Each of them had a diameter of 12 mm.

To reduce the free space between these tubes and rodlets smaller aluminium rodlets with a diameter of 5 mm were used. The final version used in SNEAK-9A-1 and SNEAK-9A-2 consisted of 12 B_4C tubes (diameter 12 mm), 4 aluminium rodlets (diameter 12 mm), and 9 aluminium rodlets (diameter 5 mm) per SNEAK element. A cross section is shown in Fig. 9.

In the follower part of the control rods normal SNEAK sodium platelets were used.

In the assembly SNEAK-9A-1 all twelve control rods were simulated in the withdrawn condition. That means, there was follower material in the core region and the lower axial blanket, and absorber material in the region of the upper axial blanket. Thus the assembly corresponded to the end of life configuration of the SNR.

Fig. 7 shows the horizontal cross section of the critical configuration and a vertical cross section through one half of the equivalent cylindrical core. For calculations in the cylindrical approximation the control rods were smeared out and mixed with normal core elements to form a cylindrical region with a thickness of about the dimensions of one control rod (see Appendix A.).

SNEAK-9A-2 was a mock up of a possible beginning of life configuration of the SNR-300. In the reference core all nine compensating rods were simulated 40 cm inserted, i.e. the boundary between absorber and follower part of the control rods was 40 cm below the upper core blanket boundary. The shut-down rods were still simulated withdrawn. The loss of reactivity by inserting the nine rods was compensated by additional core elements. The cross section of the critical configuration and a vertical cross section through one half of the equivalent cylindrical core is shown in Fig. 8.

In addition to this reference core with an insertion depths of 40/40 cm of the two control rod systems RT1 and RT2 respectively, four modifications of SNEAK-9A-2 have been built. All these cores had the same radii but only changed insertion depths of the control rods: 58/20, 28/50, 0/63, and 68/0 cm.

3. Critical experiments

Criticality calculations were performed using two different methods: The one based on a two-dimensional diffusion calculation is described in this section. The second method using the three-dimensional synthesis code KASY is described in detail in /5/.

The calculations were based on the core cross section as given in the Fig. 6 to 8. However, these configurations are slightly supercritical if in accordance with the calculational model all SNEAK shim rods are fully inserted. Table 3.1 shows the experimental results.

Table 3.1 Excess reactivities of the SNEAK-9A assemblies

Assembly	Number of SNEAK elements			Excess reactivity ρ (¢)	k_{eff}
	inner core zone	outer core zone	total		
9A-0	240	132	372	5.9	1.0004
9A-1	240 + 24+)	196 + 24+)	484	43	1.0030
9A-2/	240 + 24+)	248 + 24+)	536		
40/40				6.0	1.0004
28/50				6.9	1.0005
58/20				9.6	1.0007
0/63				4.0	1.0003
68/0				13.0	1.0009

+) simulated SNR control rods

The basis of the evaluation was to calculate the k_{eff} of the assembly in two-dimensional R-Z-geometry with the multigroup diffusion code DIXY. Then corrections for heterogeneity, cylinderization and transport effects were applied.

The main cross section set used was the 26 group set KFKINR /6/. But, to be able to compare the results to those found for previous assemblies, the k_{eff} calculations of SNEAK-9A-0 were also performed with the 26 group MOXTOT-set /7/. Using this set another correction had to be applied: The elastic scattering cross sections had to be improved by weighting them with the actual spectrum of the core under consideration (REMO-correction /8/). (For the KFKINR-set this correction is inherent for a core composition of the SNR-type.)

In Table 3.2 a comparison of the MOXTOT and KFKINR results for SNEAK-9A-0 are given. The heterogeneity correction was calculated by comparing two one-dimensional calculations with heterogeneous and homogeneous cross sections, both prepared with the cell code ZERA /9/.

The cylinderization correction was obtained by comparison of a one-dimensional calculation in cylindrical geometry and a two-dimensional calculation in X-Y-geometry. The same material and group dependent axial bucklings were used for both calculations.

The transport correction was calculated with the one-dimensional S_N-code DTK /10/ and equivalent diffusion calculations. The axial transport correction contains also the effect of the rest cell of the inner core zone elements.

Table 3.2 Comparison of the k_{eff} calculations with the KFKINR- and MOXTOT cross section set for SNEAK-9A-0

		KFKINR	MOXTOT
basic calculation 2-dim. (R-Z) DIXY	k_{eff}	0.9963	1.0109
REMO-correction	Δk	--	+ 0.0016
heterogeneity	Δk	+ 0.0060	+ 0.0067
cylinderization	Δk	- 0.0014	- 0.0015
final diffusion result	k_{eff}	1.0009	1.0177
transport correction	Δk	+ 0.0062	+ 0.0062 +)
final value	k_{eff}	1.0071	1.0239
C/E		1.0067	1.0235

+) result taken from the KFKINR calculation

Table 3.3 shows a comparison of the k_{eff} values of all critical configurations of the SNEAK-9A series. In addition to the corrections given for SNEAK-9A-0 in Table 3.2 a transport correction for the simulated SNR control rods was applied. This cor-

rection was derived from a special control rod experiment performed in SNEAK-9A-0 (see section 5.). However, the value of the correction found there, had to be adapted for each simulated SNR control rod according to the ratio of the material worths at the position under consideration and the position of the control rod in SNEAK-9A-0.

The cylinderization correction of the SNEAK-9A-2 cores was calculated separately for each core cross section with different material compositions at the simulated control rod positions (Na-follower or absorber at the positions of RT1 and RT2). These corrections were combined to the total cylinderization correction according to the fractions of the normalization integral corresponding to these axial zones. As the effect is positive for a cross section with absorber material at all control rod positions and negative for sodium follower rods, the resulting cylinderization correction includes a compensation which tends to increase the error.

The results of the synthesis calculations are also given in Table 3.3. No corrections have been applied. Therefore the results have to be compared with the results of the two-dimensional calculations plus the cylinderization corrections.

For all calculations the KFKINR cross section set was used, but the synthesis calculation were performed with only four energy groups.

Three main results can be seen from Table 3.3. First, the agreement between the synthesis calculations and the two-dimensional calculations is better than $\pm$ 0.1% except for a slightly bigger discrepancy for SNEAK-9A-1. The second remarkable result is the good agreement of all k_{eff}-values after including all corrections, as can be seen in the last row. Third, the diffusion results of all SNEAK-9A-2 cores are very similar for the synthesis calculations as well as for the two-dimensional calculations.

Table 3.3 Criticality prediction for the SNEAK-9A cores
(The k_{eff} values correspond to an experimental $k_{eff} = 1.0000$)

	SNEAK-9A-0	SNEAK-9A-1	SNEAK-9A-2[a]				
			40/40	28/50	58/20	0/63	68/0
3D synthesis KASY / 4 gr.	0.9949	0.9894	0.9931	0.9928	0.9929	0.9930	0.9929
2D (R-Z) DIXY / 26 gr.	0.9959	0.9977	0.9944	0.9950	0.9927		
Δk_{cyl}	- 0.0014	- 0.0067	- 0.0020	- 0.0026	- 0.0005		
2D (R-Z) + Δk_{cyl}	0.9945	0.9910	0.9924	0.9924	0.9922		
Δk_{het}	+ 0.0060	+ 0.0055	+ 0.0050	+ 0.0050	+ 0.0050		
Δk_{tr}	+ 0.0062	+ 0.0058	+ 0.0058	+ 0.0058	+ 0.0058		
$\Delta k_{tr,rod}$	--	+ 0.0060	+ 0.0044	+ 0.0051	+ 0.0051		
$k_{eff,corr.}$	1.0067	1.0083	1.0076	1.0083	1.0081		

a) The figures 40/40 etc. stand for the insertion depth of the inner and outer control rod bank (RT1 and RT2) in cm.

4. Calculation of the delayed neutron fraction

To be able to compare measured and calculated reactivity worths, the knowledge of the delayed neutron fraction β_{eff} is necessary. It was calculated by a perturbation calculation using two-dimensional (R-Z) diffusion fluxes with Keepin's data /13/, which are given in Tables 4.1 and 4.2 for ^{235}U and ^{238}U.

Table 4.1 Delayed and prompt fission yields and delayed neutron fractions for fast fission

Fission nuclide	Delayed neutrons per fission	$\bar{\nu}$	β
^{235}U	0.0165	2.57	0.00641
^{238}U	0.0412	2.79	0.0148

These data have been used for all SNEAK evaluations up to now, including this report. β_{eff}-calculations were performed for all critical configurations of the SNEAK-9A series, and additional for one far subcritical configuration of SNEAK-9A-2, to check the influence

Table 4.2 Delayed neutron group constants for fast fission of ^{235}U and ^{238}U

Fission nuclide	Group index	Decay constant λ_i (sec^{-1})	Relat.abundance $a_i \equiv \beta_i/\beta$	$\beta_i \cdot 10^3$
^{235}U	1	0.0127	0.038	0.244
	2	0.0317	0.213	1.365
	3	0.115	0.188	1.205
	4	0.311	0.407	2.609
	5	1.40	0.128	0.8205
	6	3.87	0.026	0.1667
^{238}U	1	0.0132	0.013	0.1924
	2	0.0321	0.137	2.028
	3	0.139	0.162	2.398
	4	0.358	0.388	5.740
	5	1.41	0.225	3.330
	6	4.02	0.075	1.110

of inserted control rods on β_{eff}. But the results given in Table 4.3 show, that there is no remarkable discrepancy between the different β_{eff}-values.

Table 4.3 β_{eff} for different core configurations calculated with Keepin's data

Core configuration	β_{eff}
SNEAK-9A-0	0.00698
SNEAK-9A-1	0.00694
SNEAK-9A-2 (40/40)	0.00689
(28/50)	0.00689
(58/20)	0.00690
(90/90/90)	0.00683

Furthermore some investigations were performed when it became clear that the mean ν-values calculated for the assembly SNEAK-9A-0 (ν_5 = 2.46 and ν_8 = 2.81) are quite different from those given by Keepin, and used up to now. Therefore a recalculation of β_{eff} was performed using the $(\nu \cdot \beta)$-values of Keepin but our own ν-values. This yielded the new value β_{eff} = 0.00719, i.e. about 3% higher than the original value. The same increase of β_{eff} was calculated at INTERATOM with one-dimensional calculations for the assemblies SNEAK-9A-1 and -9A-2. Using these higher β_{eff}-values for the evaluation of reactivity worth measurements, the C/E results would decrease by 3%.

5. The control rod experiment in SNEAK-9A-0

5.1 Scope of the experiment

A control rod experiment was performed in the clean two zone core SNEAK-9A-0 to check the calculation methods for the simulated SNR control rods in SNEAK-9A-1 and -9A-2. In particular the results of the experiment were used to improve criticality calculations of cores with control rods (see section 3.).

The main part of the investigations were performed with one central control rod (4 SNEAK elements), because there the evaluation could be done with a rather simple two-dimensional model. Afterwards some investigations with three eccentric control rods at the RT1 positions (see Fig. 7) were performed.

Because of streaming effects special interest was taken in sodium follower rods. But in replacing core material by sodium all terms, i.e. fission, absorption, diffusion, and degradation are changed considerably. Therefore the experiment was performed with the following types of elements:

Type 1 In the normal fuel elements the 20% enriched uranium platelets were replaced by natural uranium. Therefore, essentially only the fission- and absorption terms were changed.

Type 2 In the whole element - core region and both axial blankets - the normal material was replaced by sodium platelets. Now also the diffusion- and degradation terms are influenced significantly.

Type 3 Similar as type 2, but in the upper axial blanket sodium was replaced by absorber material to simulate the "withdrawn" control rod used in SNEAK-9A-1 and -9A-2.

Regarding the results of the types 1 and 2, it is possible - with some assumptions - to draw some conclusions about the discrepancies between calculation and experiment for each term separately.

5.2 Experimental results

Fig. 10 shows the configuration SNEAK-9A-0 with the positions of the one central and the three eccentrical simulated control rods. The reactivity worths were measured by the quasi critical method. For this purpose edge elements had to be added to the clean critical configuration. The excess reactivity was measured with the calibrated SNEAK shim rods. For the experiment with the one central control rod 14 elements, designed with "1" in Fig. 10, were added. For the experiment with three eccentric rods additional 18 elements - designed with a "2" - were necessary. The loading of these elements was performed stepwise, as the excess reactivity must not be greater than 1% in Δk (see Table 5.2).

In the Tables 5.1 and 5.2 the details of the experiments are given, and Table 5.3 shows the reactivity worth of each control rod type compared to the clean core.

Table 5.1 Details of the central control rod experiment

Core configuration	ρ (¢)
Clean critical + 14 edge elements (= 386 core elements)	reference
Stepwise replacement of 4 normal core elements by type 2:	
core position 17/20	- 22.7
17/19	- 21.8
18/19	- 20.6
18/20	- 20.3
total	- 85.4
Replacement of 4 elements type 2 by type 3	- 9.1
Replacement of 4 elements type 3 by type 1	- 19.7

Explanation of the element types see section 5.1.

Table 5.2 Details of the experiments with three eccentric control rods

Core configuration	ρ (¢)
Clean critical + 14 edge elements (= 386 core elements)	reference
Stepwise replacement of 4 normal core elements by type 3 at the position E1 (see Fig. 10):	
core position 15/21	- 23.5
14/21	- 20.9
15/22	- 20.7
14/22	- 18.8
total value at the position E1	- 83.9
Loading of 6 edge elements	+ 62.1
Replacement of 4 normal core elements by type 3 at the position E2	- 80.5
Loading of 8 edge elements	+ 70.8
Replacement of 4 normal core elements by type 3 at the position E3	- 77.7
Loading of 4 edge elements	+ 34.2
Replacement of 4 elements type 3 by type 1 at the position E1	- 16.5
Replacement of 8 elements type 3 by type 1 at the positions E2 and E3	- 31.9
Replacement of 4 elements type 1 by type 2 at the position E1	+ 23.3
Replacement of 8 elements type 1 by type 2 at the positions E2 and E3	+ 47.5

Table 5.3 Reactivity worths of the different control rod configurations compared to the clean core

	ρ (¢)
I. Central control rod:	
Na-follower without absorber (type 2)	- 85.4
Na-follower with absorber in the upper axial blanket (type 3)	- 94.5
U-20% replaced by U_{nat} (type 1)	- 114.2
II. Eccentric control rods:	
type 2 at position E1	- 77.1
type 2 total	- 219.7
type 3 at position E1	- 83.9
type 3 total	- 242.1
type 1 at position E1	- 100.4
type 1 total	- 290.5

Besides the comparison between the measured and calculated reactivity worths of the simulated control rods, two other results can be considered more closely.

Replacing one by one the normal core elements by type 2 elements, it is possible to get information about the self-shielding effect. From Table 5.1 one can see that the reactivity worth of the first element is approximately 6% higher than the mean value of all four elements. This result will be compared with calculations too (see section 5.4).

An indication of the mutual influence of control rods can be obtained from the eccentric control rod experiment. From Table 5.3 one can see that for all three control rod types the reactivity worth of all three control rods is about 4% - 5% lower than three times the value of the control rod at the position E1. Considering that the distance of the rod at the position E3 to the core center is 2.3 cm larger than that of the two other rods - resulting in a 4% lower reactivity worth - the self-shielding effect is certainly less than 4%. As it is not possible to calculate such a small effect accurately enough with a simple model, no self-shielding calculations have been performed in this case.

5.3 Computational methods

5.3.1 The central control rod

In general two-dimensional calculations in (R-Z)-geometry were performed. Only the self-shielding effect was calculated with one-dimensional codes in cylindrical geometry. The simulated control rod was treated as a cylinder with a radius corresponding to the correct

cross section area (radius = 6.14 cm). The following codes were used:

- the diffusion codes DIXY and 6731 of the NUSYS-system
- the transport codes SNOW /11/ and DTK /10/.

With diffusion theory k_{eff}-calculations were performed as well as first order and exact perturbation calculations. The main reason for the perturbation calculations was the splitting of the total Δk into the single terms: fission, absorption, diffusion, and degradation.

However, diffusion theory could not describe the experimental results very well for the control rod filled with sodium. Therefore two-dimensional transport calculations in (R-Z)-geometry were performed too.

To come to reasonable computing times, a compromise had to be found between the number of mesh points and the S_N-order. Fortunately it appeared that already for very few mesh points (11x9 and 22x18 respectively) the result of Δk (not k_{eff} itself!) is almost independent of the number of mesh points. It was therefore possible to use the S_6-approximation. However, S_2-calculations were also performed for reasons of comparison. The results are given in Table 5.4.

Table 5.4 Comparison of different transport calculations for one central Na-follower rod (type 2)

	11x9 mesh points		22x18 mesh points	
	S_6	S_2	S_6	S_2
k_{eff} reference	1.01027	1.01364	1.00887	1.01081
k_{eff} rod type 2	1.00420	1.00740	1.00289	1.00456
Δk	0.00607	0.00624	0.00598	0.00631
Δk C/E	1.018	1.047	1.003	1.049

5.3.2 The eccentric control rods

The basic calculation was a two-dimensional diffusion calculation in (R-Z)-geometry. The three control rods and normal core elements were smeared out to form a ring shaped zone (14.793 cm < r < 26.417 cm). A cylinderization correction was applied by comparing a one-dimen-

sional radial calculation (corresponding to the (R-Z)-calculation) and a two-dimensional (X-Y)-calculation. For both calculations the same group dependent axial bucklings were used. Finally a transport correction, derived from the central control rod, was applied for the two types control rods which had sodium in the core region.

5.4 Comparison between experiments and calculations

5.4.1 The central control rods

Table 5.5 shows the results of the calculations for the various central control rod configurations, and the comparison with the experiments. Somewhat surprising was the result for the type 1 rod (^{235}U replaced by ^{238}U), because the overestimate of about 5% is much lower than the overestimate of the ^{235}U material worth (about 11%; see section 6.). Up to now this discrepance could not be satisfactorily explained.

The main result for the sodium follower rod was the big overestimate of the experimental result by the diffusion calculation, and the good agreement with the two-dimensional transport calculation on the other hand. This may indicate a wrong calculation of the axial leakage in diffusion theory.

The result for the type 3 rod is similar to that of the type 2 rod.

Table 5.5 Comparison of the calculated and experimental reactivity worths of one central control rod

Control rod configuration	Experiment Δk [a]	Diffusion calculation DIXY (R-Z) / 26 gr.			Transport calculation SNOW S_6 (R-Z) / 26 gr.			Δk_{TR} (tr.-diff.)
		k_{eff}	Δk	Δk C/E	k_{eff}	Δk	Δk C/E	
reference	--	0.99916	--	--	1.00887	--	--	--
type 1 fuel removed	0.00797	--	0.00827 [b] 0.00835 [c]	1.038 1.048	--	--	--	--
type 2 sodium-follower	0.00596	0.99263	0.00698 [b] 0.00653 [c] 0.00659 [d]	1.171 1.096 1.106	1.00289	0.00598 [c]	1.003	- 0.00055
type 3 sodium-follower B_4C in the upper blanket	0.00660	0.99204	0.00712 [c]	1.079	1.00228	0.00659 [c]	0.999	- 0.00053

a) $\beta_{eff} = 0.698 \cdot 10^{-2}$

b) Δk from first order perturbation calculation

c) Δk from comparison of two k_{eff}-calculations

d) Δk from exact perturbation calculation

Table 5.6 Results and interpretation of the perturbation calculation for the central control rod

Reference replaced by	$\Delta k \cdot 10^3$					
	Fission	Absorption	Diffusion	Degradation	Total	C-E
type 1	- 16.37	+ 8.10	< 0.01	< 0.01	- 8.27	- 0.30
type 2	- 20.09	+ 15.35	- 1.51	- 0.34	- 6.59	- 0.63

Table 5.6 shows the results of the exact perturbation calculation for the rod configurations with removed fuel (type 1) and with sodium (type 2). For the type 1 rod diffusion and degradation are negligible. Therefore the reactivity worth is just given by the reduced fission and absorption terms. The calculation overestimates the experiment by 3.8%, i.e. $0.30 \cdot 10^{-3}$ Δk. The second row shows the calculated results for the type 2 rod (sodium follower). The overestimate of the reactivity worth is 10.6% or $0.63 \cdot 10^{-3}$ Δk.

The increased discrepancy between calculation and measurement is most probably due to an overestimate of the axial diffusion by about 25%.

Table 5.7 Comparison of the experimental and calculated self-shielding effect of the central sodium follower rod

$\frac{\Delta k \text{ (4 normal core elements replaced by 4 elements type 2)}}{4 \times \Delta k \text{ (1 normal core element replaced by 1 element type 2)}}$		
Experiment	1-dim. calculations	
	Diffusion	Transport, S_8
0.940	0.961	0.948

The self-shielding effect of one sodium follower rod is shown in Table 5.7. It is defined by the ratio of the reactivity worth of the whole control rod (4 SNEAK elements) and four times the worth of the first normal core element replaced by one sodium follower element. The effect is relatively small - about 6% - and is fairly well reproduced by the calculations.

5.4.2 Three eccentric control rods

The comparison of the calculations with the experiments is given in Table 5.8. As there appeared no significant difference between the type 2 and type 3 results in the central case (see Table 5.5), the calculations for the eccentric case were performed only for the type 1 and type 2 control rods.

Table 5.8 Comparison of the experimental and calculated reactivity worths of three eccentric control rods

Control rod configuration reference replaced by	Experiment	Calculations				
			Corrections			
	Δk	Δk [a)]	Δk_{cyl}	Δk_{tr} [b)]	Δk_{corr}	C/E
type 1	0.02028	0.02084	-0.00013	--	0.0207	1.020
type 2	0.01534	0.01697	+0.0009	-0.0014	0.0165	1.076

a) Comparison of two k_{eff}-diffusion calculations in (R-Z)-geometry

b) Derived from the last column of Table 5.5

The result for the three type 1 control rods is in a very good agreement with the result of the central control rod. On the other hand there is still a remarkable overestimate of the reactivity for the sodium follower rods. The reason for this may be a too small transport correction, which was derived from the central control rod. However, in the core center the diffusion term is only given by the axial diffusion effect, as there is no radial flux gradient, while at the eccentric positions also the radial diffusion effect is to be regarded.

Probably this is the main reason for the overestimate of the eccentric control rod worth. In order to yield the same C/E ratio, the transport

correction should have about twice the value derived from the central experiment. This was therefore assumed for the control rod transport correction in the k_{eff}-calculations of SNEAK-9A-1 and -9A-2 (see section 3.).

5.5 Comparison with former control rod experiments

Control rod experiments have already been performed in the assemblies SNEAK-2C, SNEAK-6A, and SNEAK-6D /1/, /12/. Obviously one should compare these results with the recent ones of SNEAK-9A. Unfortunately an exact comparison is not possible. On the one hand the composition of the control rods was not identical in all cases, on the other hand different calculational models and cross section sets have been used.

Nevertheless in Table 5.9 the C/E ratios are given for the reactivity worth of a central sodium follower rod. Neglecting the details one can see, that all diffusion calculations overestimate the reactivity worth of the control rods by approximately 10%. The worse agreement of the SNEAK-2C result is probably due to the smaller core height and the therefore greater influence of the diffusion term.

On the other hand the two-dimensional transport calculations are in a very good agreement with the experiments.

The influence of the cross section set depends slightly on the calculational model used, as was shown in /12/. However, there is no remarkable difference between the MOXTOT- and the KFKINR-results in the case of the sodium follower rod in SNEAK-9A-0, calculated with 26 groups and the two-dimensional diffusion code DIXY in (R-Z)-geometry.

Table 5.9 Comparison of the central control rod experiments in the assemblies SNEAK-2C, -6A, -6D, and -9A-0

Cross section set	Calculational model	Δk C/E			
		2C [1]	6A [2]	6D [3]	9A-0 [4]
NAPPMB	DIXY R-Z 4 gr. KASY 4 gr. SNOW S_4 4 gr.	1.24	1.09 1.11 1.01	1.12	
MOXTOT	DIXY R-Z 26 gr. DIXY R-Z 4 gr.			1.065 1.08	1.091
KFKINR	DIXY R-Z 26 gr. SNOW S_6 26 gr.				1.094 1.003
Core height (cm)		60.3	89.4	89.4	90.0
Replaced fuel		Pu	Pu	Pu	Uranium

Composition of the control rods:

1) U_{depl} in the lower axial blanket, sodium between the lower core-blanket boundary and 20 cm above the upper core-blanket boundary, above this B_4C.

2) Breeder blanket in the lower axial blanket, sodium in the upper axial blanket and the core region.

3) Breeder blanket in both blanket zones, MASURCA-sodium in the core region.

4) Sodium in the whole control rod.

6. Material worth determination

6.1 Experiment

The material worth measurements in SNEAK-9A-0 were performed with the pile oscillator (see /14/), which was positioned at one of the four central core element positions. The upper part of the pile oscillator consists of several boxes, each containing the equivalent of 15 SNEAK-platelets 1/8" thick. In order to accomodate in these boxes a composition similar to the inner zone, the unit cell was modified slightly by omitting the graphite platelet.

In the central box a Na_2CO_3-platelet was replaced by a Al (40%) and a Al_2O_3-platelet in order to establish suitable sample positions (see Fig. 5).

In most cases the samples were introduced in place of the Al-40%-platelet, the Na-value was measured by replacing the Na-platelet with an empty box, some samples could be introduced between the platelets. In all cases the material worth was corrected to give the value for the clean sample material.

The reactivity change during the oscillation was compensated by an automatic control rod, which was calibrated before, using the inverse kinetic equations. The sample worth was then derived from the control rod positions, which were recorded by a computer during the whole measurement.

Table 6.1 Material worths in SNEAK-9A-0

Sample		Reactivity worth (m$/gr)			Relative values to ^{235}U		
Main isotope	Weight (g)	Experiment	Calculation	C/E	Experiment	Calculation	C/E
^{235}U	6.64	0.243 ± 0.004	0.2705	1.11	1.000	1.000	1.00
^{238}U	122.67	-0.0193 ± 0.0002	-0.0203	1.05	-0.079	-0.0749	0.95
^{239}Pu	4.06	0.340 ± 0.01	0.373	1.10	1.40	1.38	0.99
^{240}Pu	2.70	0.046 ± 0.01	0.0554	1.20	0.19	0.205	1.08
^{241}Pu	1.24	0.460 ± 0.01	0.523	1.14	1.89	1.93	1.02
Na	10.0	-0.006 ± 0.002	-0.0032	0.53	-0.025	-0.0118	0.47
^{10}B	0.589	-8.49 ± 0.15	-7.98	0.94	-34.9	-29.50	0.85
^{10}B (B_4C)	0.891	-8.61 ± 0.10	-8.105	0.94	-35.4	-29.96	0.85
B_4C	6.26	-1.225 ± 0.02	-1.170	0.95	-5.04	-4.33	0.86

6.2 Calculation

The material worths were first calculated with a perturbation calculation using two-dimensional fluxes of a DIXY-(R-Z)-calculation and homogeneous cross sections (generated with the NUSYS program Nr. 446). Afterwards a heterogeneity correction was applied, taking into account the resonance self-shielding of the cross sections in the real platelet structure. This correction was calculated with the KAPER-program /15/, /16/, which determines the material worth of small samples by exact perturbation theory (using the perturbed adjoint fluxes for each sample). Two KAPER-calculations were performed for each sample: one with heterogeneous and one with homogeneous cross sections. The heterogeneity correction is given by the ratio of both results (see Table 6.2) and is added to the homogeneous DIXY material worth. This procedure was used to overcome difficulties with the normalization integral.

Table 6.2 Heterogeneity corrections for the calculated material worths

Isotope	$\frac{HET - HOM}{HOM}$ (%)
^{235}U	- 1.0
^{238}U	- 9.8
^{239}Pu	+ 1.0
^{240}Pu	+ 4.1
^{241}Pu	- 1.3
Na	+ 10.3
^{10}B	- 9.2
B_4C	- 6.5

6.3 Comparison of calculation and experiment

The experimental and the calculated results are given in Table 6.1. The comparison shows an overestimate of the reactivity worth for all fissile materials of 12±2%. The result of the ^{240}Pu material worth is not very conclusive. Because of the small sample the measured reactivity worth was very small too and therefore the accuracy was rather bad. The same is true for the Na-worth. The worth of ^{10}B and B_4C respectively is slightly underestimated, which is in a good agreement to the control rod experiments in SNEAK-9A-2.

7. Reaction rate measurements

7.1 Experimental techniques

The main reason for the reaction rate measurement in SNEAK-9A-0 was to compare various fine structure calculations with the experimental results. Therefore, the axial fission rate distribution through the unit cell of ^{235}U and ^{238}U and the capture rate of ^{238}U were measured with metal foils. These foils were positioned partly between SNEAK-platelets and partly within special perforated fuel platelets (see Fig. 11). The absolute reaction rates were obtained by relating the foil results to the counting rate of absolute calibrated parallel plate fission chambers /17/, and - for the ^{238}U capture rate - by comparing the γ-count rate of the foils with that of a calibrated ^{243}Am source /18/, /19/.

The horizontal fine structure was obtained by scanning an irradiated SNEAK fuel platelet.

7.2 Calculations

The following types of calculations have been performed:

a) Comparison of the cell fine structure calculated with the codes ZERA /10/, KAPER /15/, /16/, and REAC. For this purpose the unit cell was subdivided into 15 regions (each fuel platelet was subdivided into 5 regions).

b) Comparison of the calculated results with the experimental ones. For this purpose a macro cell of 5 unit cells was investigated, comprising four normal unit cells and one cell containing all foils according to the experiment. This calculation was performed with the REAC code, using the KFKINR cross section set.

c) To check the influence of the cross section set an additional calculation of the same kind as b) was performed with the REAC code and the ENDF/B-III cross section set.

7.3 Experimental and calculated results

In Table 7.1 the reaction rate distribution in the central unit cell is given relative to the reaction rates between the two parallel plate fission chambers. Also given are the cell average results. A correction for the horizontal fine structure was only found for the fission rate of ^{238}U .

Table 7.1 Reaction rate distribution within the central unit cell of SNEAK-9A

Position	$^{235}U_{fission}$	$^{238}U_{fission}$	^{238}U capture
Parallel plate chamber	1.000	1.000	1.000
1	1.159	1.144	1.183
2	1.163	1.183	1.164
3	1.151	1.204	1.041
4	1.163	1.181	1.146
5	1.161	1.153	1.150
6	1.156	1.186	1.127
7	1.147	1.203	1.031
8	1.160	1.183	1.154
9	1.160	1.147	1.179
Cell average	1.154	1.195 1.183+)	1.066

+) With a correction for the horizontal fine structure

The spectral indices are given in Table 7.2 together with the calculated results. One can see that the calculated results obtained with the KFKINR cross section set are very similar for all codes, but for F8/F5 a discrepancy of about 5% was found between the results from the KFKINR and the ENDF/B-III cross section set.

Table 7.2 Measured and calculated spectral indices in the center of SNEAK-9A-0

			F8/F5	C8/F5
Experiment			0.0275±0.0005	0.136±0.004
Calculation	KFKINR	KAPER	0.0262	0.136
		ZERA	0.0261	0.136
		REAC	0.0260	0.134
	ENDF/B-III	REAC	0.0273	0.135

Comparing the calculated results with the measurements a very good agreement is found for the C8/F5 index. On the other hand the F8/F5 index is remarkably underestimated by all calculations using the KFKINR cross section set (about 5%). Only the result using the ENDF/B-III set is in a good agreement with the experiment.

The Fig. 12 and 13 show the reaction rate distribution calculated with various codes[+]. The same normalization was used in all cases, i.e. the mean reaction rate in both fuel platelets is equal to 1.0.

Generally the following statements can be made:

- within the fuel platelets the discrepancies are in each case, lower than 1%,

- the shape of the F5-fine structure calculated with ZERA is apparently wrong,

- the F8-fine structure is calculated remarkably higher with KAPER then with ZERA,

- there is no significant discrepancy between the KAPER and REAC result for capture of ^{238}U.

The Fig. 14 to 16 show the comparison between the measured fine structure and the REAC-calculations. The following conclusions can be drawn:

[+] In order to give a better survey the rates were also plotted through sodium and structural material using cross sections for infinite dilution in these parts of the cell.

- the reaction rate shift between the two fuel platelets calculated for F5 was less pronounced in the experiment,

- the fine structures of the ^{238}U reaction rates are remarkably underestimated for fission as well as for capture.

If one looks again at Fig. 12 one can see that apparently the experimental fission fine structure would be better predicted with the KAPER than with the REAC code. However, no code is able to calculate the right C8 fine structure within the fuel platelets.

Using the ENDF/B-III cross section set for the fine structure calculation, no important influence was recognized for the fission rate distribution, even if the spectral index was changed significantly. However the capture rate fine structure was less marked than using the KFKINR set.

8. Determination of the material buckling

The experimental value of the material buckling of the inner core zone of the SNEAK-9A-0 assembly was deduced from four fission rate traverses (^{235}U, ^{238}U, ^{239}Pu, and ^{237}Np) in both the axial and radial direction. From these traverses the fundamental modes were deduced using calculated weighting functions according to a method originally suggested by Meyer-Heine et al. /20/ and later on improved in Cadarache and Karlsruhe /21/.

For the determination of the radial buckling an additional cylinderization correction was applied to take into account irregularities caused by the SNEAK shim rods, and the core boundary.

For the calculation of the material buckling the following definition was chosen in order to be consistent with the k_{eff}-calculations:

The calculated buckling is defined as the buckling which yields $k_{eff} = 1$, using a zero-dimensional calculation with homogeneous cross sections and adding heterogeneity and REMO corrections. The calculation was performed with the MOXTOT and the KFKINR cross section sets.

Table 8.1 Experimental results of the buckling measurements in SNEAK-9A-0

axial buckling α (m^{-1})	2.525 ± 0.005
radial buckling β (m^{-1})	2.762 ± 0.010
material buckling $B_m^2 = \alpha^2 + \beta^2$	14.01 ± 0.06

In Table 8.1 the experimental results are given. The quoted errors are statistical ones, and do not contain systematic errors, which may be somewhat larger, especially for the radial buckling.

In Table 8.2 the calculated results and the C/E-values are given for the KFKINR and the MOXTOT cross section sets. The overestimate

Table 8.2 Calculated material buckling for the inner core zone of SNEAK-9A-0

	MOXTOT	KFKINR
Δk_{het}	+ 0.0074	+ 0.0066
Δk_{REMO}	+ 0.0016	--
$k_{eff,homogeneous}$	0.9910	0.9934
B_m^2 (m^{-2})	16.12	15.01
C/E	1.151	1.071

of the experimental value is rather larger for both cross section sets. But comparing the results to former ones one notes a certain consistency. On the one hand the KFKINR result is the same as for SNEAK-7B and similar to those of SNEAK-7A and SNEAK-9B. On the other hand the 8% higher MOXTOT result is about consistent to the 1.7% higher k_{eff}-value obtained with the MOXTOT cross section set.

Nevertheless the reasons for the general bad agreement between measured and calculated material buckling should be further investigated.

Appendix A

Atomic compositions used for the SNEAK-9A assemblies

For the calculations of the SNEAK-9A assemblies it was necessary to introduce a large number of different compositions, since in addition to the clean cell compositions a variety of mixtures had to be used in order to take into account SNEAK shim rods, simulated SNR control rods as well as rest cells and different types of element tubes.

In the following tables each composition is identified by a letter and up to three numbers.

For core mixtures this identification code has the general form:

C y n z

where C stands for core

y is a number indicating the core zone
(1. inner zone
2. outer zone)

n characterizes the inclusion of rest cells and of SNEAK shim rods

z indicates the inclusion of simulated SNR control rods
(1. with follower material
2. with absorber material)

Blanket compositions are identified by a code of the form

B x n z

where B stands for blanket

x indicates the blanket zones
(1. inner axial blanket
2. outer axial blanket
3. radial blanket)

n characterizes the type of element tubes involved or the mixing ratio with simulated SNR control rod compositions

z indicates if absorber or follower material is used for the SNR rods
(1. follower
2. absorber)

The presence of SNEAK shim rods in the blanket region has a small effect and was not especially taken into account.

A detailed summary of all mixtures is given in Table A.1. The atomic densities of the core mixtures can be taken from Table A.2 and of the blanket mixtures from Table A.3.

Table A.1a Summary of all core mixtures of the SNEAK-9A assemblies

Notation	Definition						Used in 9A-0	Used in 9A-1	Used in 9A-2
C 1	clean cell of the inner zone						x	x	x
C 2	clean cell of the outer zone						x	x	x
C 001	SNR control rod, follower part						x	x	x
C 002	SNR control rod, absorber part						x	x	x
	combination of								
	normal elements		elements of SNEAK control rods		elements of SNR control rods				
	inner zone	outer zone	inner zone	outer zone	follower part	absorber part			
C 10	22							x	x
C 101	44				12			x	
C 102	44					12		x	
C 11	226		14				x	x	x
C 121	42		2		12				x
C 122	42		2			12			x
C 131	60		8		12			x	x
C 132	60		8			12		x	x
C 14	100		6					x	
C 15	102		4						x
C 21		126		6			x		
C 221		84		4	24			x	x
C 222		84		4		24		x	x
C 23		106		2				x	
C 24		157		3					x
C 25		190		6				x	
C 26		241		7					x

Table A.1b Summary of all blanket mixtures of the SNEAK-9A assemblies

Notation	Definition					Used in 9A-0	Used in 9A-1	Used in 9A-2
B 1	inner axial blanket					x	x	x
B 2	outer axial blanket					x	x	x
		number of elements in element tubes version						
		C	B					
B 30	radial blanket	204	365			x		
B 31	radial blanket	164	478				x	
B 32	radial blanket	130	460					x
	combination of							
	normal elements		elements of SNR control rods					
	inner axial blanket	outer axial blanket	follower part	absorber part				
B 111	44		12				x	x
B 112	44			12			x	x
B 211		44	12				x	x
B 212		44		12			x	x
B 121	68		12				x	x
B 122	68			12			x	x
B 221		68	12				x	x
B 222		68		12			x	x

Table A.2 Atomic compositions (10^{22} atoms/cm^3) for the core mixtures of the SNEAK-9A assemblies

Isotope \ Mixture	C 1	C 2	C 001	C 002	C 10	C 101	C 102	C 11	C 121	C 122
Al				2.1170	0.006897	0.005421	0.4587	0.06257	0.03952	0.4927
B 10				0.4091			0.087671			0.087671
B 11				1.6787			0.3597			0.3597
C	1.0495	1.4590	0.003721	0.5233	1.0450	0.8221	0.9333	1.0456	0.8225	0.9337
Cr + Mn	0.2666	0.2527	0.3171	0.1196	0.2665	0.2773	0.2351	0.2691	0.2789	0.2366
Fe	0.9072	0.8569	1.0769	0.3984	0.9069	0.9433	0.7979	0.9151	0.9483	0.8030
H	0.002599	0.001189			0.002621	0.002060	0.002059	0.002606	0.002051	0.002051
K	0.000273	0.000125			0.000276	0.000217	0.000217	0.000275	0.000216	0.000216
Mg					0.000071	0.000056	0.000056	0.000641	0.000405	0.000405
Mo	0.001514	0.001706	0.002415	0.000997	0.001509	0.001703	0.001399	0.001420	0.001648	0.001345
Na	1.2729	1.1385	1.6671		1.2724	1.3569	1.0000	1.2353	1.3342	0.9773
Nb	0.000854	0.000854	0.000854	0.000854	0.000854	0.000854	0.000854	0.000804	0.000824	0.000823
Ni	0.1485	0.1477	0.1854	0.05724	0.1482	0.1562	0.1287	0.1485	0.1564	0.1278
O	1.0026	0.4587	0.000031		1.0113	0.7948	0.7946	1.0087	0.7932	0.7932
Si	0.01144	0.01159	0.01621	0.00863	0.01147	0.01249	0.01086	0.01197	0.01279	0.01117
Ti								0.000228	0.000139	0.000139
U 235	0.14892	0.23979			0.14738	0.11582	0.11582	0.14763	0.11598	0.11598
U 238	0.59392	0.43933			0.58777	0.46192	0.46192	0.58879	0.46258	0.46258

Table A.2 continued

Isotope \ Mixture	C 131	C 132	C 14	C 15	C 21	C 221	C 222	C 23	C 24	C 25	C 26
Al	0.1013	0.4184	0.06092	0.04292	0.04317	0.03392	0.4876	0.01759	0.01781	0.02908	0.02681
B 10		0.061370					0.087671				
B 11		0.2518					0.3597				
C	0.8900	0.9677	1.0456	1.0454	1.4593	1.1474	1.2587	1.4591	1.4591	1.4592	1.4592
Cr + Mn	0.2785	0.2488	0.2690	0.2682	0.2535	0.2671	0.2248	0.2530	0.2530	0.2532	0.2532
Fe	0.9464	0.8446	0.9148	0.9122	0.8589	0.9056	0.7602	0.8577	0.8577	0.8582	0.8581
H	0.002203	0.002203	0.002607	0.002611	0.001184	0.000930	0.000930	0.001187	0.001187	0.001185	0.001186
K	0.000233	0.000232	0.000275	0.000275	0.000125	0.000098	0.000098	0.000125	0.000125	0.000125	0.000125
Mg	0.001037	0.001032	0.000624	0.000440	0.000442	0.000347	0.000344	0.000180	0.000182	0.000298	0.000275
Mo	0.001493	0.001281	0.001423	0.001451	0.001628	0.001797	0.001493	0.001675	0.001674	0.001654	0.001658
Na	1.2679	1.0182	1.2364	1.2484	1.0995	1.2212	0.8639	1.1226	1.1224	1.1123	1.1143
Nb	0.000768	0.000769	0.000806	0.000822	0.000815	0.000824	0.000824	0.000838	0.000838	0.000828	0.000830
Ni	0.1543	0.1351	0.1485	0.1484	0.1471	0.1553	0.1278	0.1474	0.1474	0.1473	0.1473
O	0.8555	0.8553	1.0088	1.0096	0.4578	0.3597	0.3597	0.4583	0.4583	0.4581	0.4581
Si	0.01303	0.01189	0.01195	0.01179	0.01189	0.01281	0.01119	0.01171	0.01171	0.01179	0.01177
Ti	0.000390	0.000388	0.000221	0.000147	0.000178	0.000140	0.000139	0.000072	0.000073	0.000120	0.000110
U 235	0.12573	0.12573	0.14762	0.14754	0.23968	0.18831	0.18831	0.23974	0.23974	0.23971	0.23972
U 238	0.50150	0.50150	0.58877	0.58843	0.43916	0.34503	0.34503	0.43926	0.43926	0.43921	0.43922

Table A.3 Atomic compositions (10^{22} atoms/cm^3) for the blanket mixtures of the SNEAK-9A assemblies

Mixture / Isotope	B 1	B 2	B 30	B 31	B 32	B 111	B 112	B 211	B 212	B 121	B 122	B 221	B 222
Al	0.2615	1.4263	0.3320	0.3836	0.4019	0.2055	0.06583	1.1222	1.5736	0.2223	0.5392	1.2135	1.5294
B 10							0.087671		0.087671		0.061369		0.061369
B 11							0.3597		0.3597		0.2518		0.2518
C	0.004530	0.002044	0.000483	0.000347	0.000299	0.004357	0.1157	0.002402	0.1132	0.004409	0.08219	0.002294	0.08023
Cr + Mn	0.2685	0.2190	0.04259	0.03062	0.02637	0.2789	0.2366	0.2399	0.1977	0.2758	0.2462	0.2336	0.2041
Fe	0.9074	0.7255	0.1408	0.1012	0.08714	0.9436	0.7983	0.8004	0.6554	0.9327	0.8312	0.7779	0.6764
H	0.000615					0.000484	0.000483			0.000523	0.000523		
K													
Mg	0.002886	0.009645	0.002415	0.002791	0.002924	0.002269	0.002268	0.007588	0.007578	0.002454	0.002453	0.008206	0.008198
Mo	0.001956	0.000997	0.000355	0.000255	0.000220	0.002054	0.001750	0.001299	0.000997	0.002025	0.001812	0.001209	0.000997
Na	0.6653					0.8796	0.5230	0.3555		0.8152	0.5657	0.2487	
Nb	0.000874	0.000854	0.000304	0.000219	0.000188	0.000870	0.000870	0.000854	0.000854	0.000871	0.000871	0.000854	0.000854
Ni	0.1439	0.1152	0.06156	0.05587	0.05383	0.1527	0.1253	0.1301	0.1027	0.1501	0.1309	0.1256	0.1065
O	1.3979	1.1597				1.0989	1.0984	0.9124	0.9124	1.1887	1.1886	0.9867	0.9857
Si	0.01445	0.01496	0.002354	0.002015	0.001895	0.01483	0.01320	0.01522	0.01360	0.01471	0.01358	0.01514	0.01401
Ti		0.001818	0.000038	0.000043	0.000046			0.001430	0.001428			0.001546	0.1545
U 235	0.004992	0.005828	0.016245	0.016245	0.016245	0.003925	0.003925	0.004585	0.004585	0.004245	0.004245	0.004959	0.004959
U 238	0.68833	0.80313	3.9940	3.9940	3.9940	0.54110	0.54110	0.63189	0.63189	0.58529	0.58529	0.68331	0.68331

References

/1/ F. Helm et al.

Physics Investigations of Sodium Cooled Fast Reactors SNEAK-Assembly 2

KFK-1399 (June 1971)

/2/ G. Jourdan et al.

Physics Investigations of Sodium Cooled Fast Reactors SNEAK-Assemblies 6A/6B

KFK-1612 (June 1972)

/3/ Ph. Hammer and F. Plum

Physics Investigations of Sodium Cooled Fast Reactors Core Z1 MASURCA in SNEAK-Assembly 6D

KFK-1581, CEA-N-1561 (September 1972)

/4/ G. Jourdan et al.

Physics Investigations of Sodium Cooled Fast Reactors SNEAK-Assembly 9B - Part 1

KFK-report in preparation

/5/ M. Pinter et al.

Control rod worth and power distribution measurements in the SNR mock up SNEAK-assembly 9A

KFK-report in preparation

/6/ E. Kiefhaber

The KFKINR-Set of Group Constants; Nuclear Data Basis and First Results of its Application to the Recalculation of Fast Zero-Power Reactors

KFK-1572 (March 1972)

/7/ E. Kiefhaber and J.J. Schmidt

Evaluation of Fast Critical Experiments Using Recent Methods and Data

KFK-969 (September 1970)

/8/ H. Küsters et al.

The Group Cross Section Set KFK-SNEAK; Preparation and Results

KFK-628 (October 1967)

/9/ D. Wintzer

Zur Berechnung von Heterogenitätseffekten in periodischen Zellstrukturen thermischer und schneller Kernreaktoren

KFK-743 (Januar 1969)

/10/ C. Günther und W. Kinnebrock

Das eindimensionale Transportprogramm DTK

KFK-1381 (März 1971)

/11/ C. Günther und W. Kinnebrock

SNOW, Ein zweidimensionales S_N-Programm zur Lösung der Neutronentransportgleichung in Platten- und Zylindergeometrie

KFK-1826 (Juli 1973)

/12/ S. Pilate, F. Plum

Control Rod Experiments in SNEAK-Assembly 6

KFK-1633 (July 1972)

/13/ G.R. Keepin

Physics of nuclear kinetics

Addison - Wesley Publishing Company, Inc. 1965

/14/ W.J. Oosterkamp

The measurement and calculation of the reactivity worth of samples in a fast heterogeneous zero power reactor

KFK-1036 (September 1969)

/15/ P.E. Mc Grath, E.A. Fischer

Calculation of Heterogeneous Fluxes, Reaction Rates and Reactivity Worths in the Plate Structure of Zero Power Fast Critical Assemblies

KFK-1557 (March 1972)

/16/ P.E. Mc Grath

KAPER - Lattice Program for Heterogeneous Critical Facilities (User's Guide)

KFK-1893 (December 1973)

/17/ R. Böhme et al.

Messung von Reaktionsraten im schnellen Nulleistungs-reaktor SNEAK

atw Juli 1971, S. 360

/18/ E. Korthaus et al.

Zur Messung von Spalt- und Einfangraten mit Spaltspur-detektoren und Ge(Li)-Detektoren

Reaktortagung Bonn 1971, S. 50

/19/ H. Seufert, D. Stegemann

A Method for Absolute Determination of U-238 Capture Rates in Fast Zero Power Reactors

Nucl. Sci. Eng. 28, p. 277-285 (1967)

/20/ A. Meyer-Heine et al.

Analysis of Experiments performed in MASURCA

BNES Conference, London 1969, Paper 1.2

/21/ H. Küsters et al.

Progress in Fast Reactor Physics in the Federal Republic of Germany

KFK-1632 (August 1973) p. 5.20

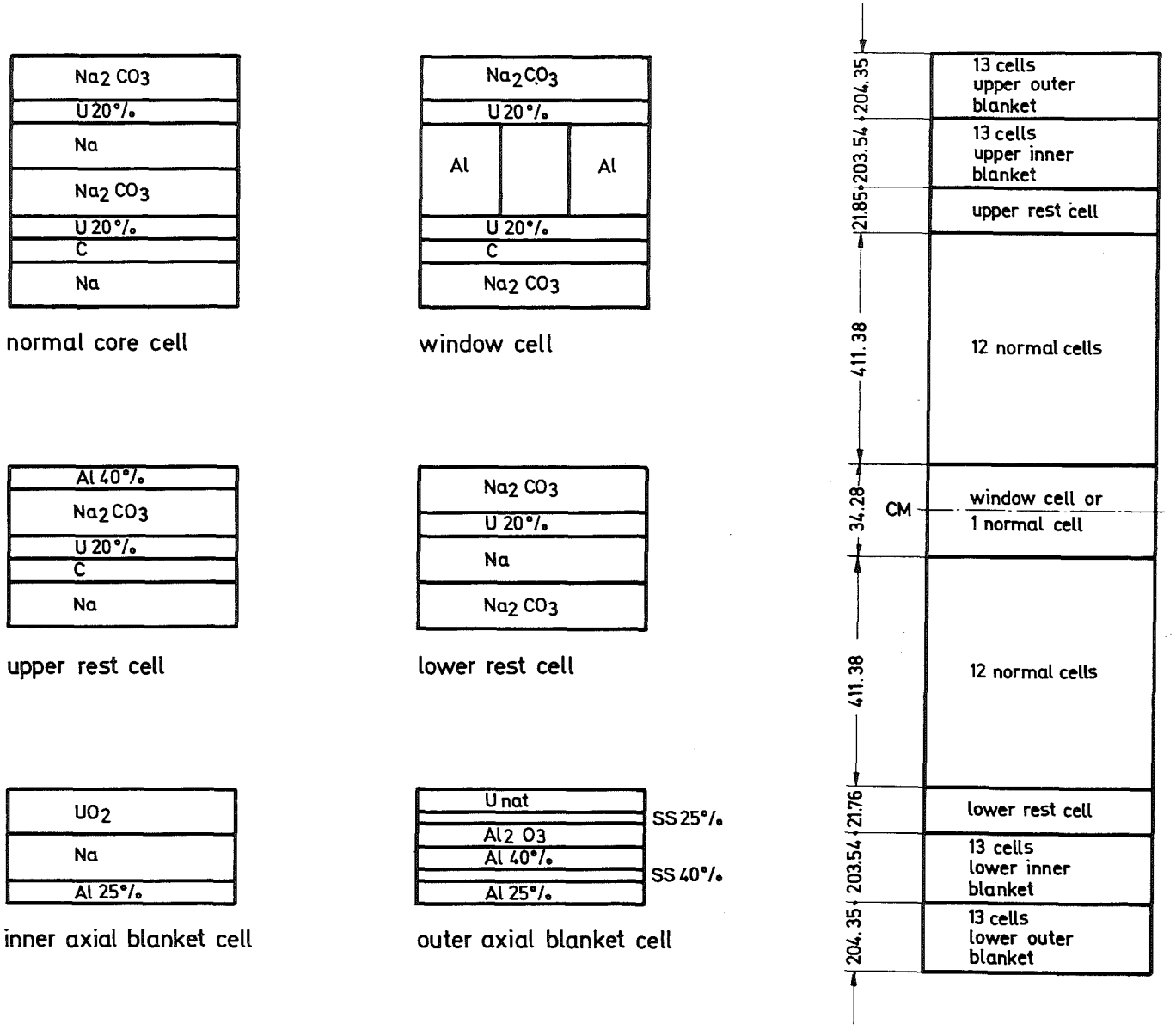

height of the cells :

normal cell	34.28 mm
upper rest cell	21.85 "
lower rest cell	21.76 "
inner axial blanket	15.66 "
outer axial blanket	15.72 "
height of the core	900.66 "
height of the blanket	407.89 "
total height of one element	1716.44 "

Fig. 1 Cells and Structure of Normal- and Window Elements of the inner Core Zone of SNEAK - 9A

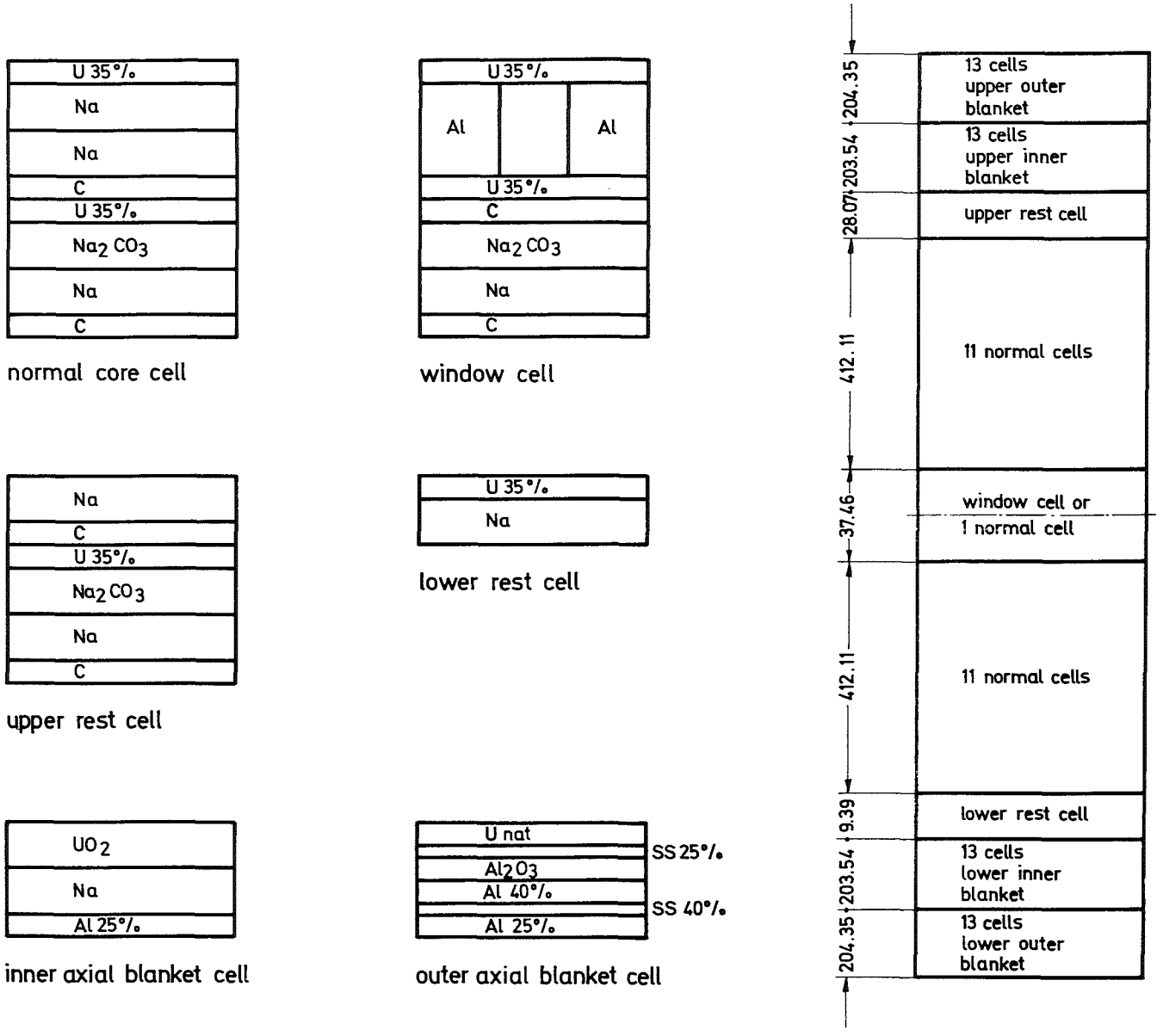

height of the cells :

normal cell	37.46 mm
upper rest cell	28.07 "
lower rest cell	9.39 "
inner axial blanket	15.66 "
outer axial blanket	15.72 "
height of the core	899.14 "
height of the blanket	407.89 "
total height of one element	1714.92 "

Fig.2 Cells and Structure of Normal-and Window Elements of the outer Core Zone of SNEAK-9A

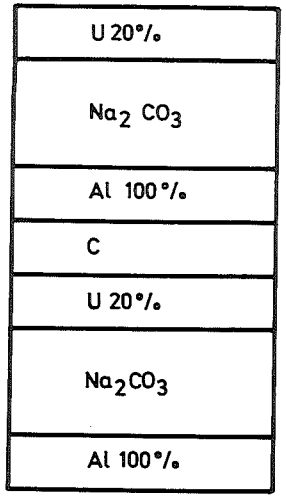

normal cell

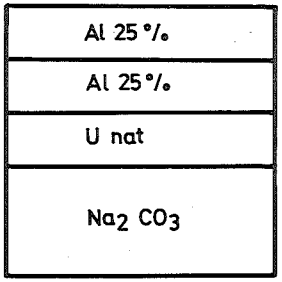

inner axial blanket cell of the safety rod

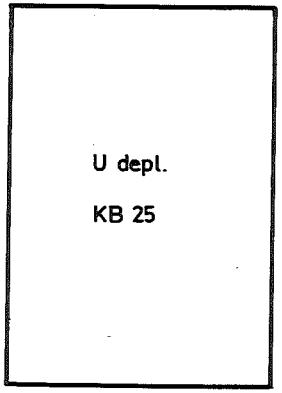

outer axial blanket cell

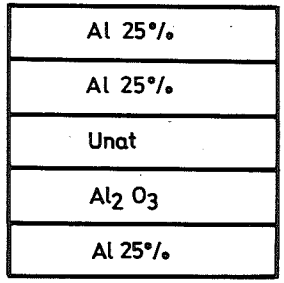

inner axial blanket cell of the shim rod

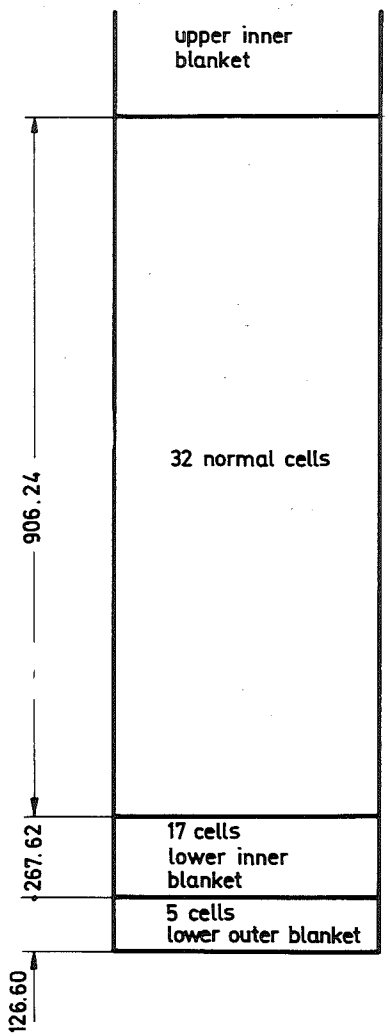

height of the cells :	
normal cell	28.32 mm
inner axial blanket	15.74 "
outer axial blanket	25.32 "
height of the core	906.24 "
height of the lower blanket	
shim rod	394.22 "
safety rod	~200 "

Fig. 3 Cells and Structure of the SNEAK-9A Shim- and Safety Rods of the inner Core Zone

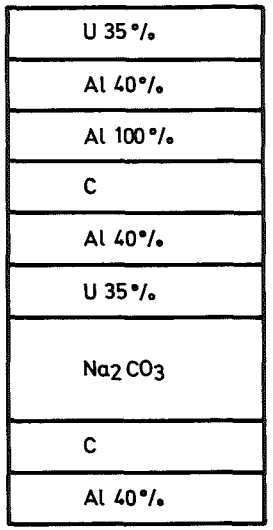

normal cell

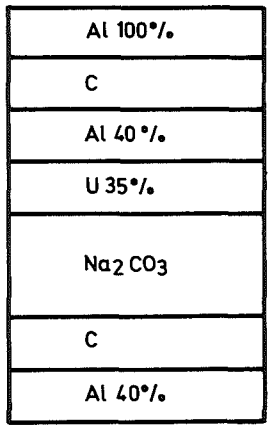

upper rest cell

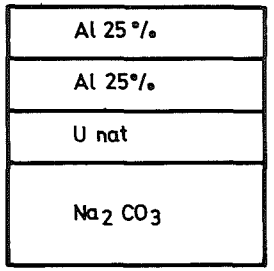

inner axial blanket cell of the safety rod

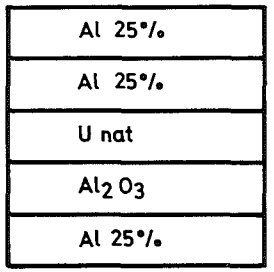

inner axial blanket cell of the shim rod

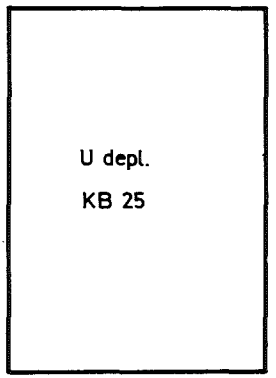

outer axial blanket cell

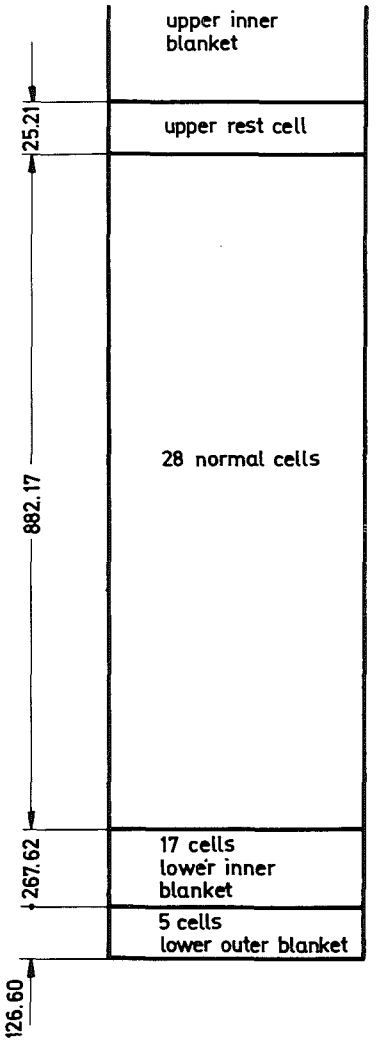

height of the cells :

normal cell	31.51 mm
upper rest cell	25.21 "
inner axial blanket cell	15.74 "
outer axial blanket cell	25.32 "
height of the core	907.38 "
height of the lower blanket	
shim rod	394.22 "
safety rod	~ 200 "

55

Fig. 4 Cells and Structure of the SNEAK-9A Shim- and Safety Rods of the outer Core Zone

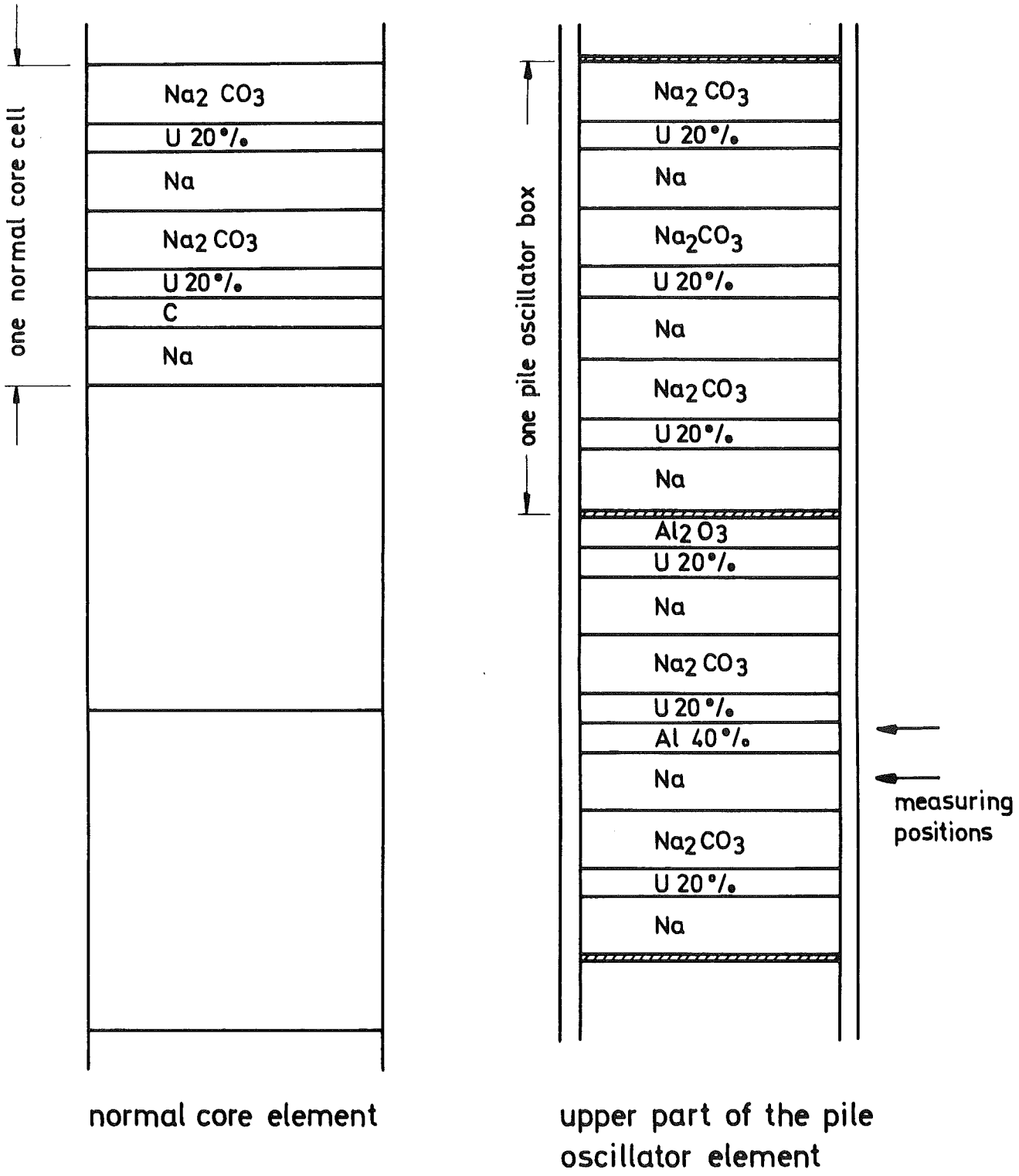

Fig.5 Arrangement of the Platelets in the upper Part of the Pile Oscillator Element compared with a Normal Core Cell

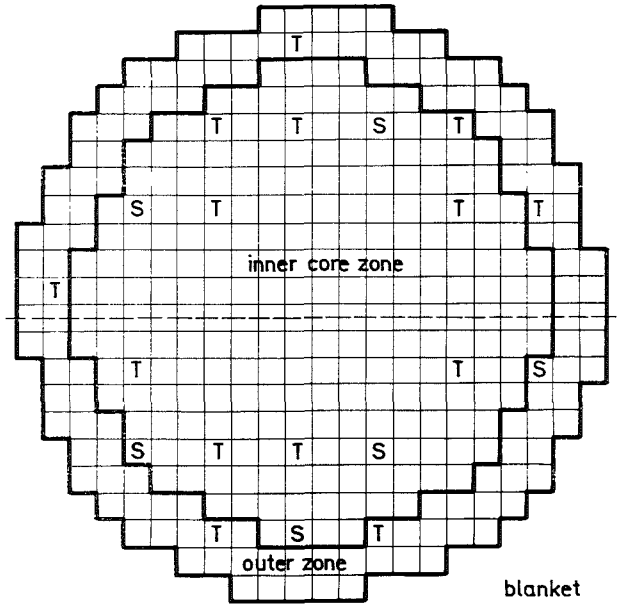

S = safety rod
T = shim rod

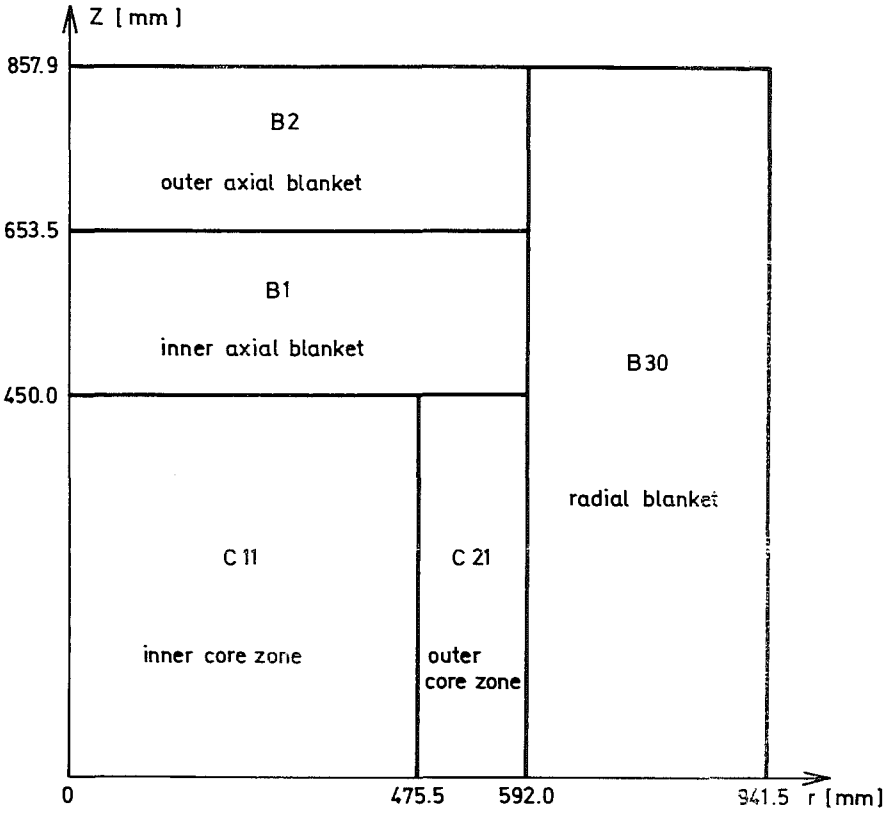

Fig. 6 SNEAK-9A-0 Critical Configuration and Vertical Cross Section through one Quarter of the Equivalent Cylindrical Core

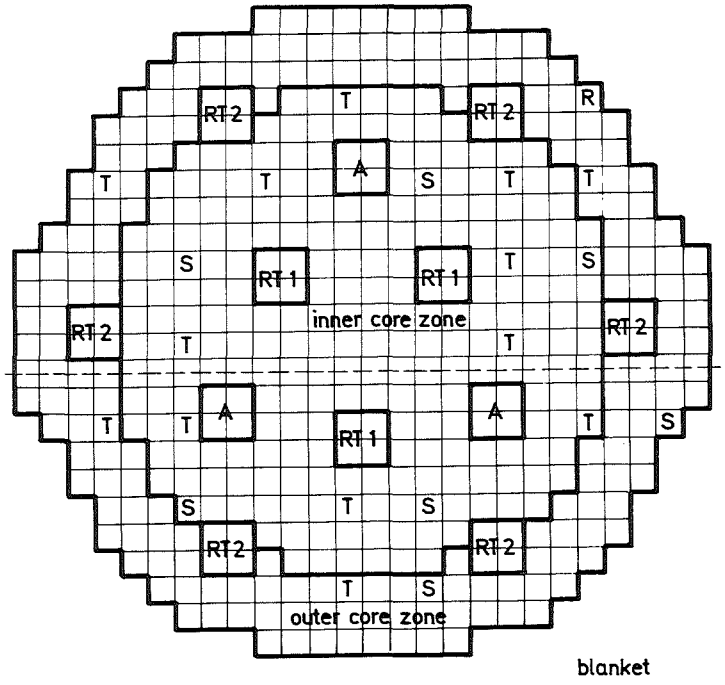

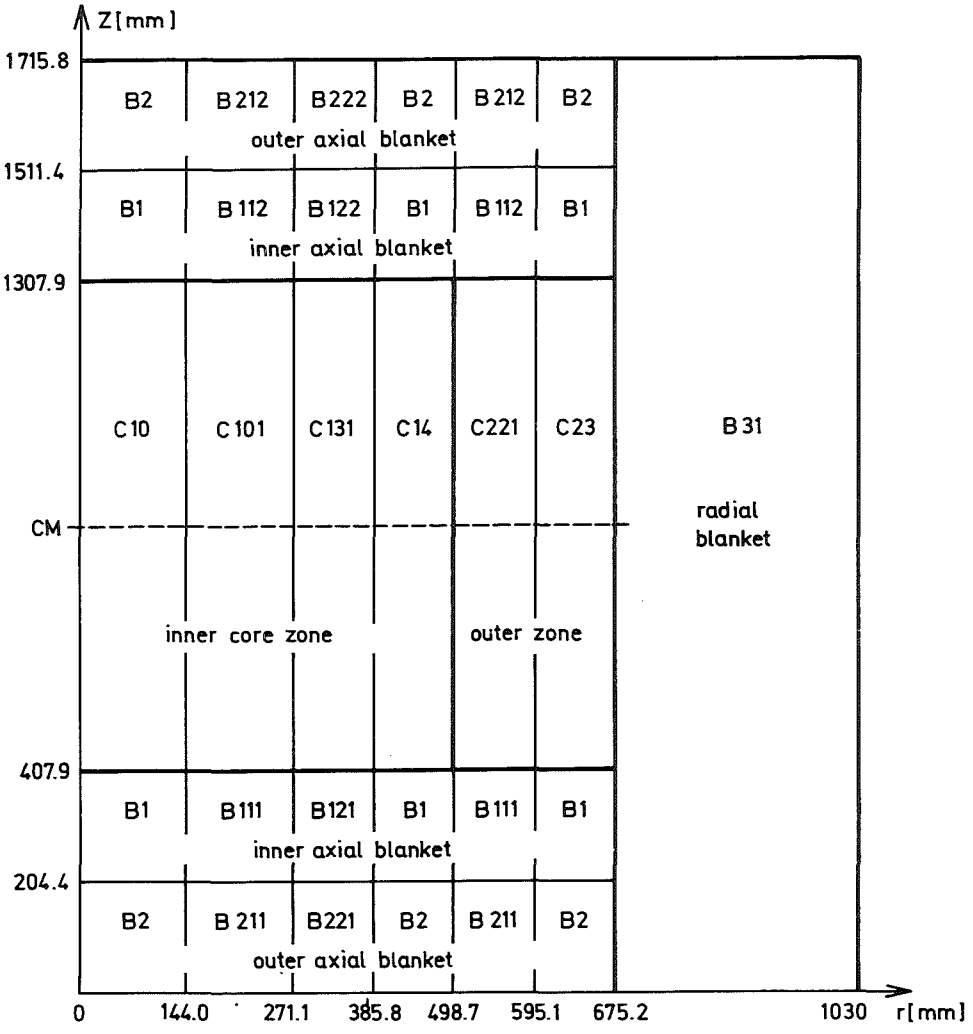

S = safety rod
T = shim rod
R = regulating rod
A = simulated SNR safety rod (withdrawn)
RT1, RT2 = simulated SNR regulating rod (withdrawn)

Fig.7 SNEAK - 9A-1 Critical Configuration and Vertical Cross Section through one Half of the Equivalent Cylindrical Core

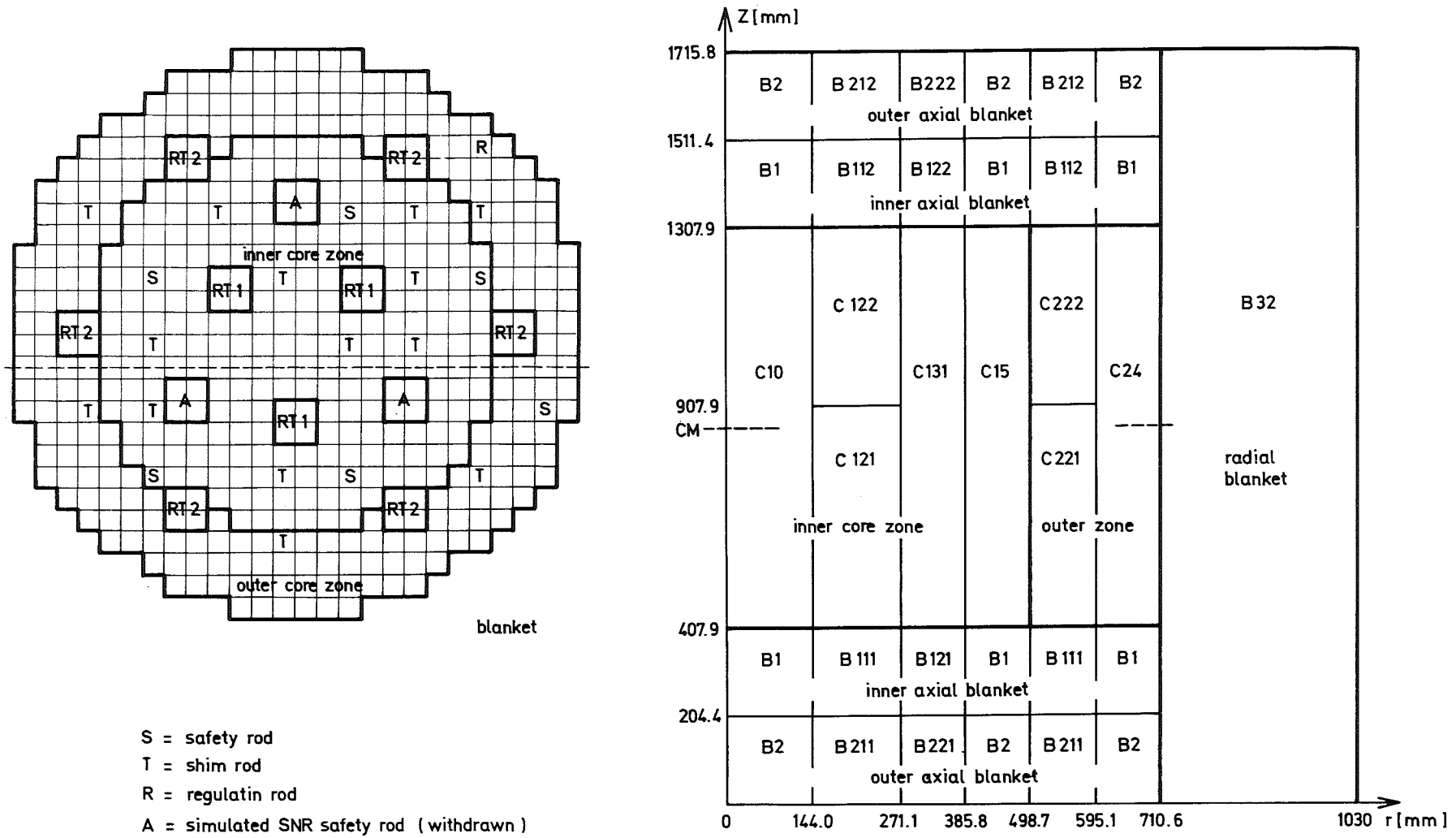

Fig.8 SNEAK - 9A-2 Critical Configuration and Vertical Cross Section through one Half of the Equivalent Cylindrical Core

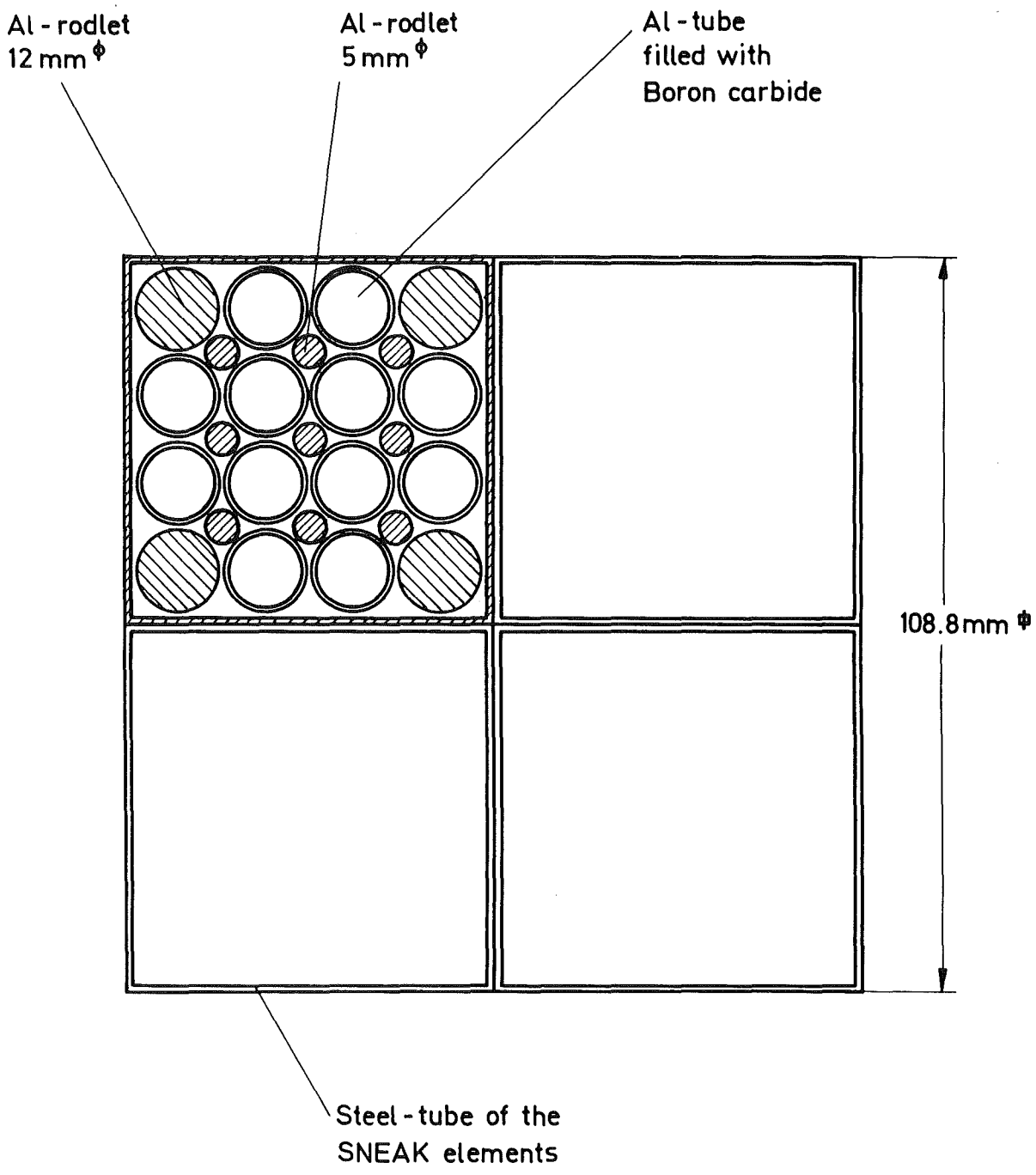

Fig. 9 Cross Section through a SNR - Control Rod, simulated by 4 SNEAK - Elements

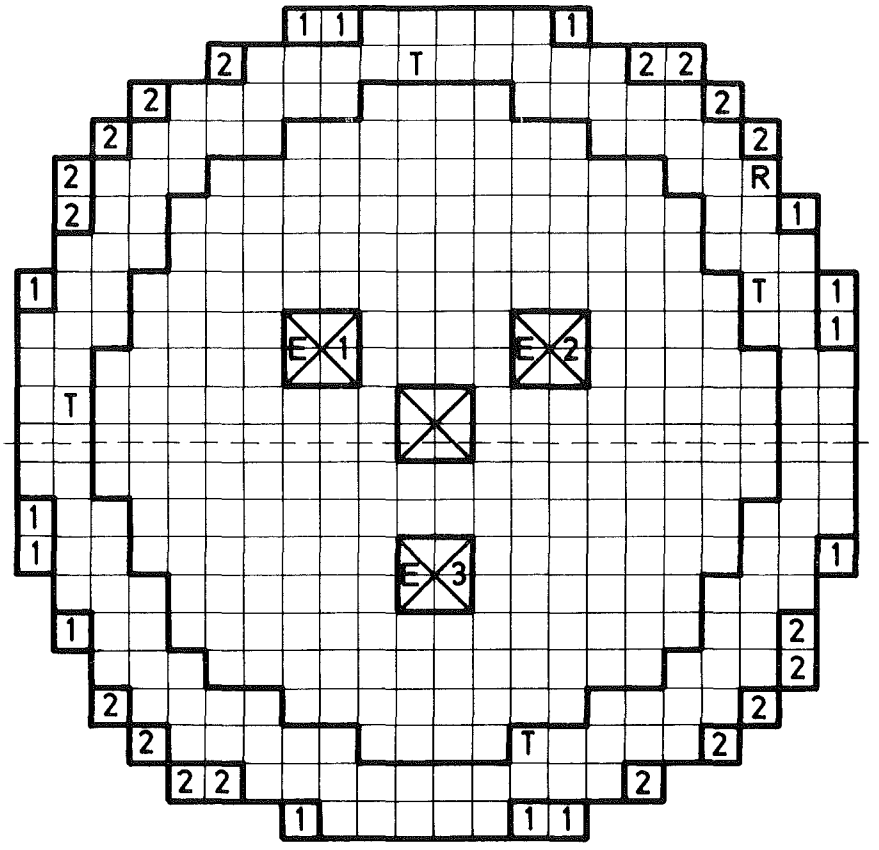

simulated control rod

T calibrated SNEAK - shim rods

R calibrated SNEAK - control rod

1,2 edge elements added to the clean critical

Fig. 10 SNEAK - 9A-0 with one Control and three eccentric simulated Control Rods respectively

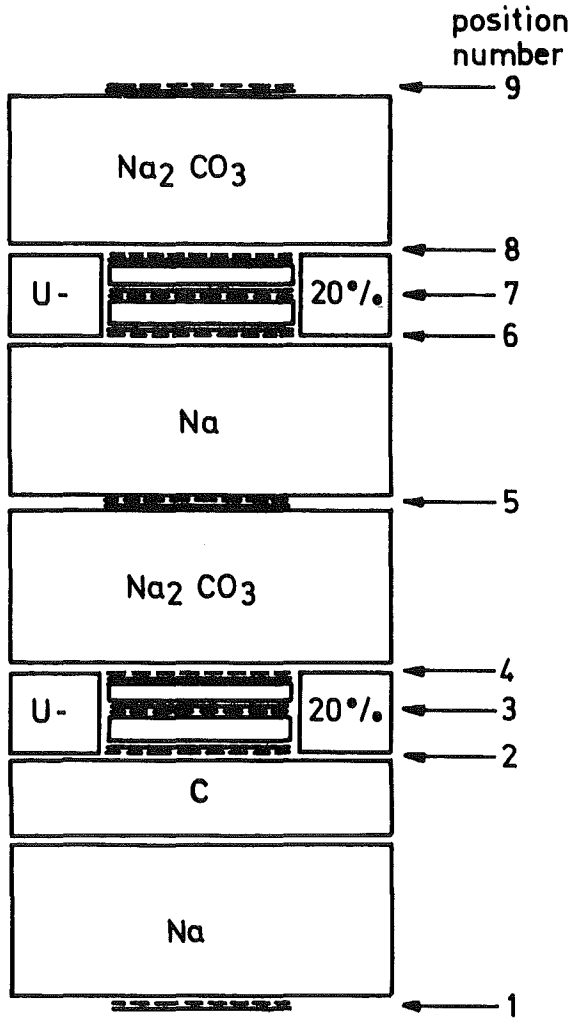

——————— foil of depleted Uranium (0.43 % U 235)

——————— foil of enriched Uranium (20 % U 235)

Fig. 11 Unit Cell of the inner Core Zone of SNEAK-9A-0 with Foils for the Reaction Rate Measurement

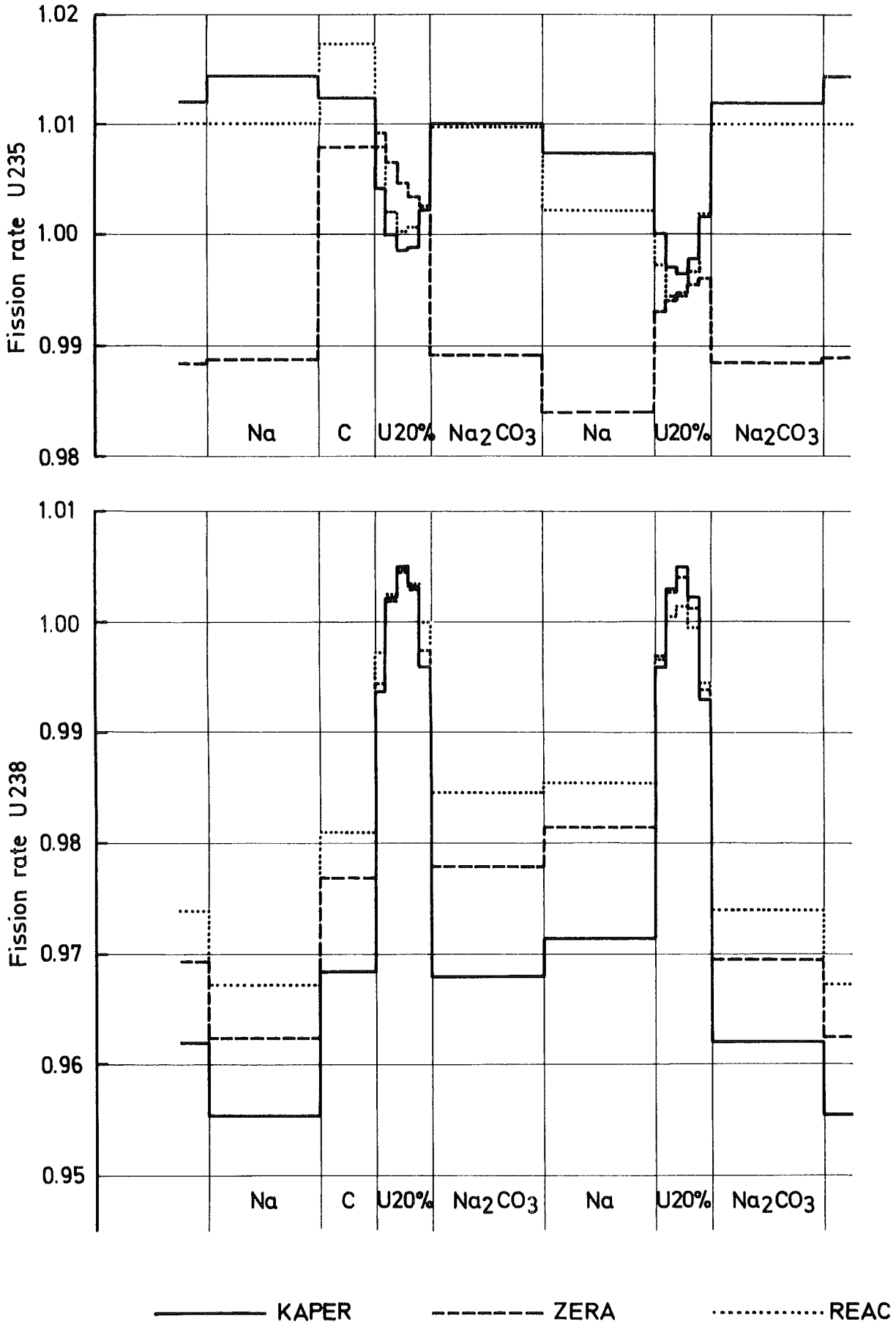

Fig.12 Fission Rate fine Structures in the Unit Cell of SNEAK-9A calculated with various Codes

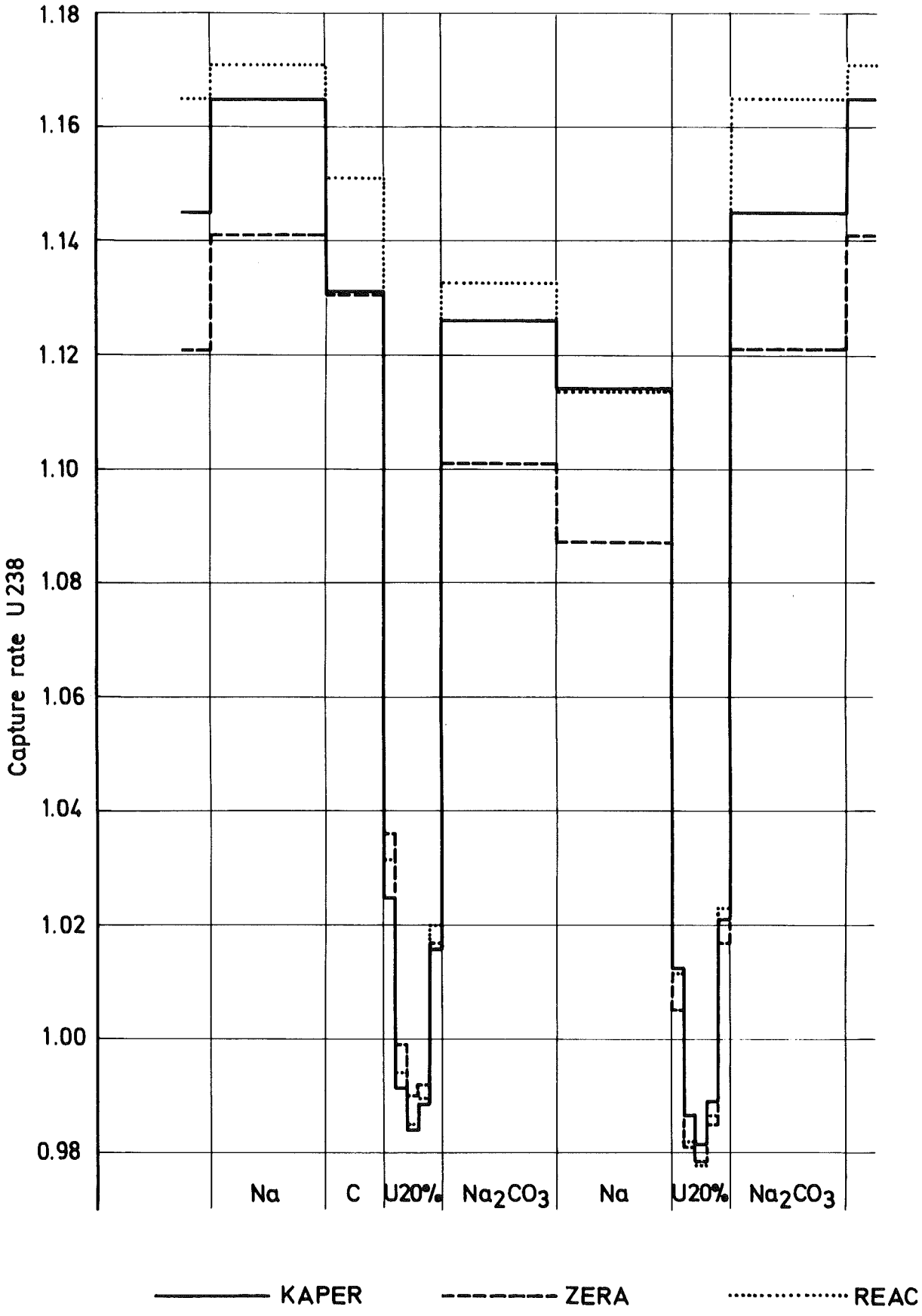

Fig.13 Capture Rate fine Structure in the Unit Cell of SNEAK-9A calculated with various Codes

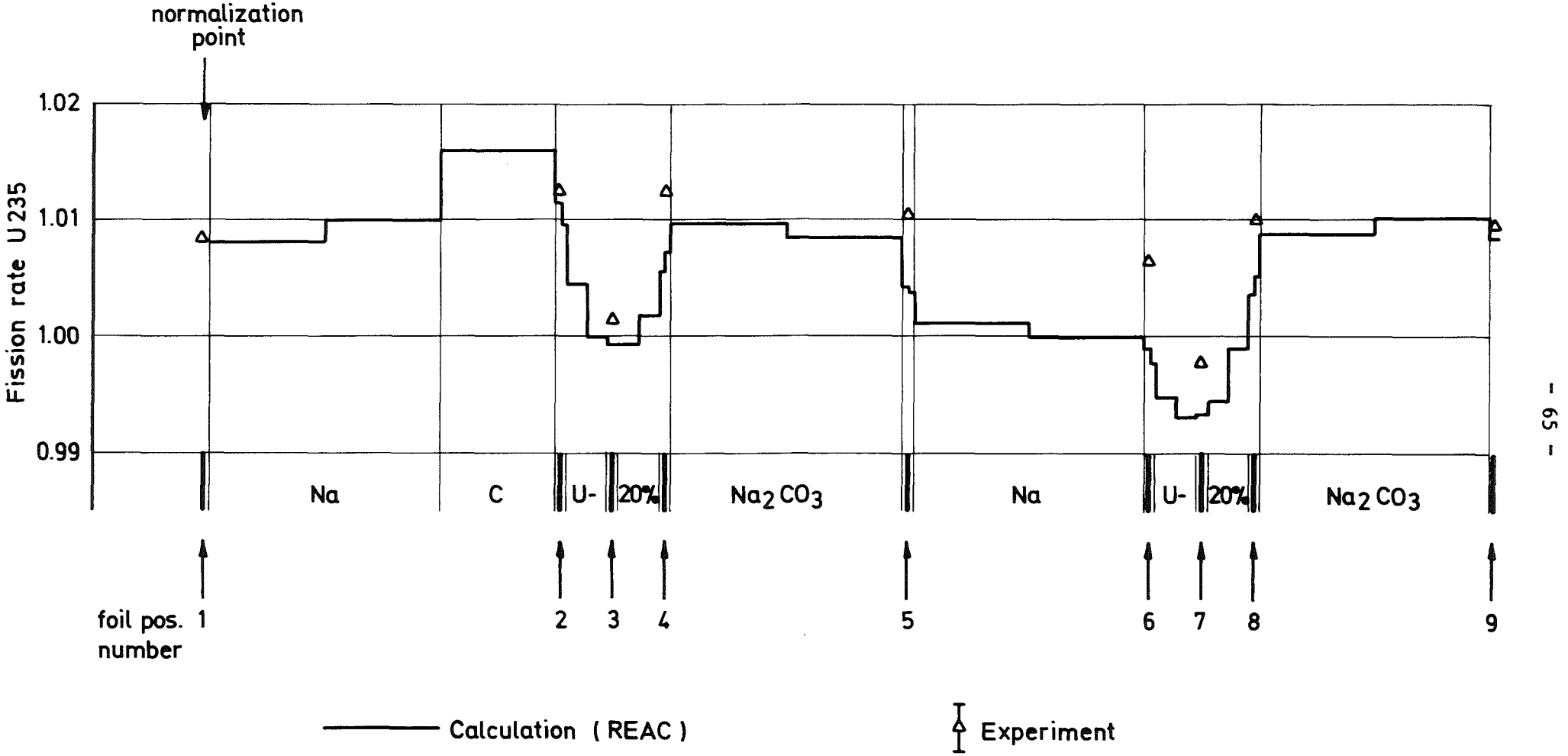

Fig.14 Comparison of calculated and measured Fission Rate fine Structure of U235 in the Central Unit Cell of SNEAK - 9A

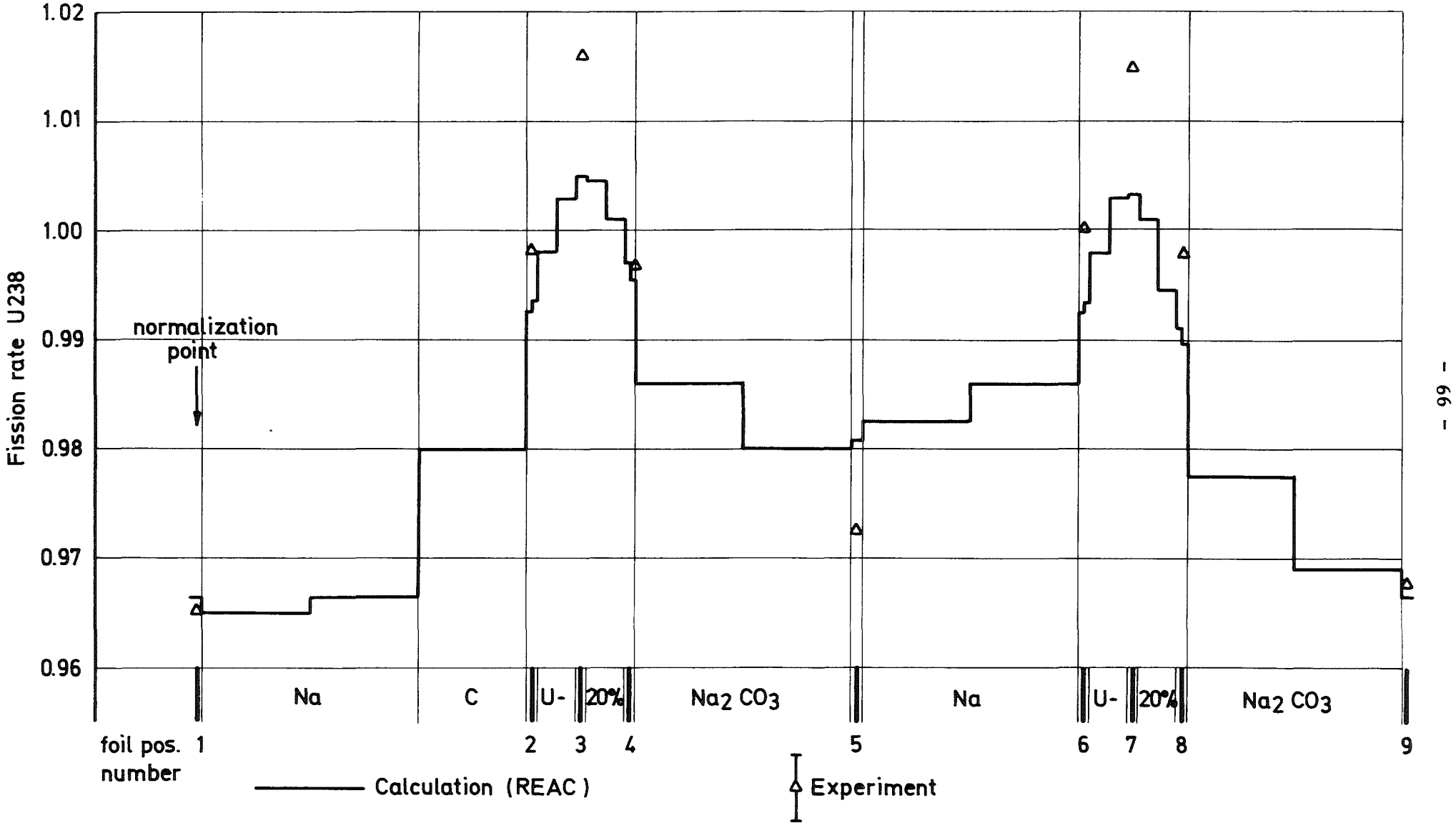

Fig.15 Comparison of calculated and measured Fission Rate fine Structure of U238 in the Central Unit Cell of SNEAK-9A

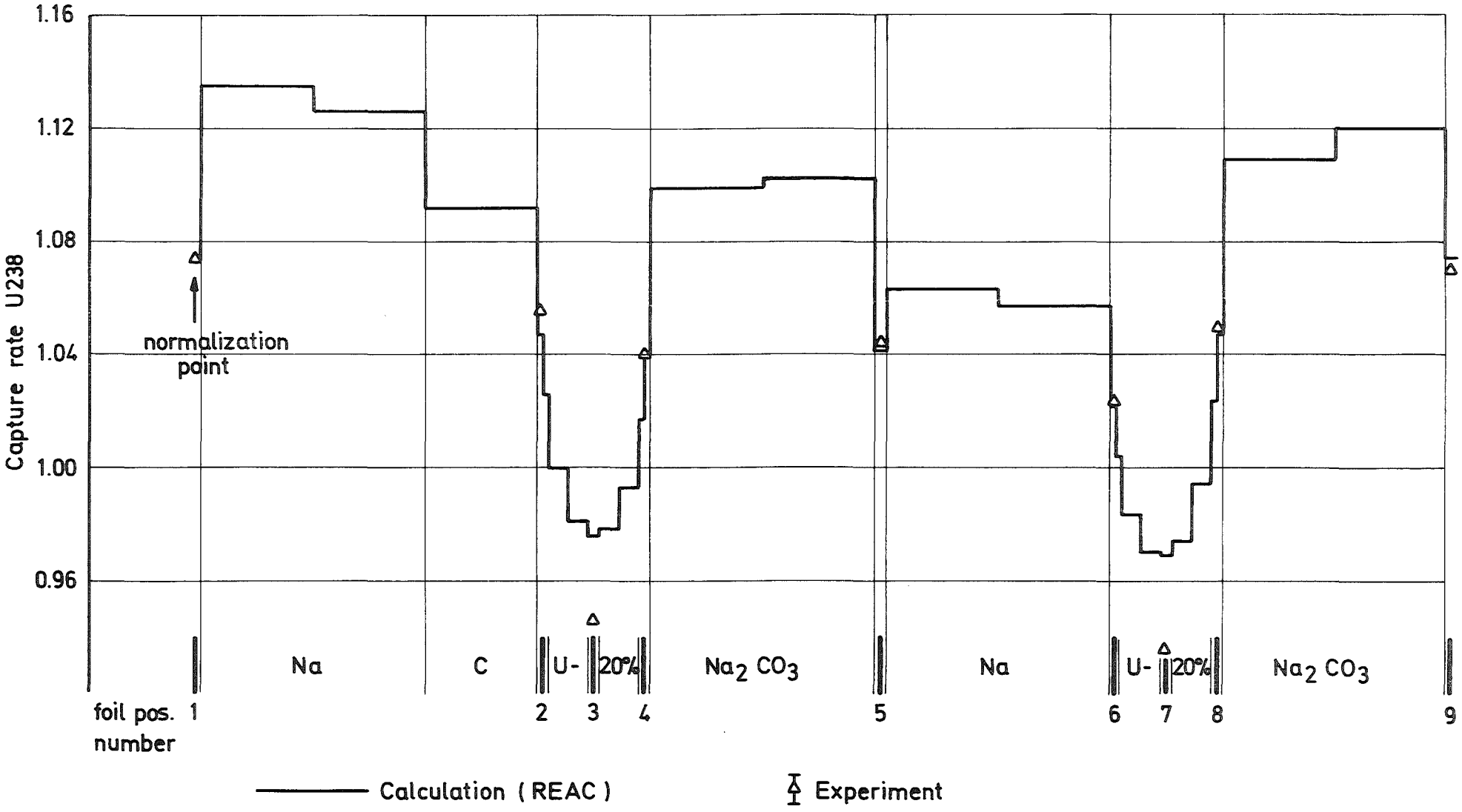

Fig. 16 Comparison of calculated and measured Capture Rate fine Structure of U238 in the Central Unit Cell of SNEAK - 9A